Article

Prospects of Graphene-Based Materials in E-Fuel Applications

Raphael Mmaduka Obodo [1,2,3,4,5,6]
https://orcid.org/0000-0001-7418-8526
raphael.obodo@unn.edu.ng
raphael.obodo@uaes.edu.ng

Hope E. Nsuade [2]

Joseph N. Anosike [7]
https://orcid.org/0009-0007-6899-4768

Imosobomeh L. Ikhioya [2]
https://orcid.org/0000-0002-5959-4427

Chimezie U. Eze [2,8]
https://orcid.org/0000-0002-1009-2741

Miletus O. Duru [8]
https://orcid.org/0009-0003-0708-2379

Joseph N. Aniezi [1]
https://orcid.org/0000-0002-1653-7692

Ekwevugbe Omugbe [1]
https://orcid.org/0000-0003-1510-4235

Chinonso Mbamara [1]

Ugochukwu C. Elejere [2,9]
https://orcid.org/0000-0001-6426-1865

Abdoulaye Diallo [10]
https://orcid.org/0000-0002-4984-1076

Ishaq Ahmad [3,4,5,6]
https://orcid.org/0000-0002-6573-0392

1 Department of Physics, University of Agriculture and Environmental Sciences, Nigeria.
2 Department of Physics and Astronomy, University of Nigeria.
3 National Centre for Physics, Quaid-i-Azam University, Pakistan.
4 NPU-NCP Joint International Research Centre on Advanced Nanomaterials and Defects Engineering, Northwestern Polytechnical University, China.
5 UKM-NCP Joint Research and Development Centre, Universiti Kebangsaan Malaysia.
6 Institute of Microengineering and Nanoelectronics, Centre of Excellence in Physics, Quaid-i-Azam University, Pakistan.
7 Department of Pure and Industrial Chemistry, University of Nigeria.
8 Department of Physics, University of Ilorin, Nigeria.
9 Department of Physics, Federal College of Education, Nigeria.
10 Department of Physics and Chemistry, Faculty of Sciences and Technologies of Formation and Education, Cheikh Anta Diop University, Senegal.

UNISA university of south africa PRESS
Nano-Horizons
Volume 3 | 2024 | 16430 | 44 pages

Nano-Horizons
https://doi.org/10.25159/3005-2602/16430
ISSN 3005-2602 (Online)

Abstract

In recent years, research studies on e-fuels such as e-methane, e-kerosene, e-methane, e-ammonia, e-diesel and e-methanol have engrossed the interest of scientists because of their unique features. These fuels are in vapour or molten phase that are formed from renewable energy sources (such as solar, wind and water) or decarbonised electricity. Recent research studies on the fabrication and applications of e-fuels have advanced significantly owing to the integration of graphene and its derivatives with special chemical and physical characteristics in their various working principles and applications. The most recent developments in the fabrication and applications of materials that are graphene-based e-fuels include the integration of graphene in electrodes and electrolytes of the e-fuel devices. E-fuels are also used in the decarbonisation of our environment since anthropogenic carbon (IV) oxide (CO_2) and carbon (II) oxide (CO) emitted from various sources will be reduced; consequently reducing greenhouse effects. This review aims at exploring techniques of using graphene and its derivatives in enhancing the performance and elongating the lifespan of e-fuel devices.

Keywords: Application, efficiency, e-fuels, graphene, lifespan, performance, prospects.

1 Introduction

Providing sufficient and adequate energy for the ever-growing human population, which will meet both industrial and household needs, has been a major concern to scientists [1], [2], [3]. The natural resources such as coal, oil and natural gas that provide energy have almost been depleted, and the extraction of energy from them has a detrimental impact on the environment [4], [5], [6]. Although the production of energy from renewable sources has a significantly smaller impact on the environment, several disadvantages, such as greater costs and worse efficiency, exist [7], [8]. This shortcoming prompted research into extremely efficient energy sources, such as e-fuels. The consensus is that e-fuels will eventually replace fuels used in some human activities, especially transportation [9], [10].

The explosive growth in e-fuel applications over the last ten years provides insight into the significance of e-fuels. An electrochemical process takes place in an e-fuel device to produce electricity. Through redox processes, it transforms the chemical energy of an oxidising agent and a fuel into electrical energy [10], [11]. E-fuels have a far better efficiency than combustion cells since their chemical energy is converted into electricity through a chemical reaction; the only by-product that remains is water [12]. E-fuels do not require charging because they can generate power as long as fuel is available. E-fuels can operate at up to 85% efficiency if the waste heat is managed well [13], [14]. The components of an e-fuel device includes bipolar plates (BPs), a cathode, an anode and an electrolyte. The oxidation of the fuel takes place at the anode while oxygen

reduction reactions (ORRs) occur at the cathode. These are the two primary processes involved in the working principle of an e-fuel device [15]. The electrochemical performance, efficiency, economic viability and stability are some of the issues when choosing material for the components of e-fuel devices [16], [17]. Conducting polymers and non-porous graphitic carbon are the most recent two main components used in BPs. Two electrodes encircle an electrolyte layer in a conventional e-fuel device. To lower oxygen (O_2) at the cathode, fuels are normally oxidised at the anode surfaces and the liberated electrons travel through outside circuits. To complete the circuit, the mobile charge transporters (H^+, OH^-, CO_3^{2-} or O^{2-}) pass through the electrolytes concurrently [18] [19].

The selection of materials for the components of e-fuel systems has issues related to the electrochemical performance, stability and productivity [20]. Graphene and its derivatives are attractive materials for e-fuel applications owing to their superior mechanical, electrical and chemical properties. Recently, much research has been done to maximise the probable applications of graphene and its derivatives in e-fuel devices. Materials based on graphene are excellent electrocatalysts because they enhance the quantity of active sites and make it easier for electrons to move during the ORR and fuel oxidation [21], [22]. It has been shown that metal-free graphene materials are desirable ORR candidates because of their inexpensive cost, strong electrocatalytic activity and high poisoning tolerance [23]. Extensive studies have been conducted on the ways in which the efficiency of e-fuel devices is affected by graphene defects, doping configurations, electronic structure modification and functional groups [24], [25], [26].

Graphene-based components added to polymer membranes enhance ionic conductivity and reduce fuel crossover [6]. Materials based on graphene show promise as high-proton conductivity and exchange membranes that are impervious to methanol, water and H_2 [27], [28]. Graphene-based materials can enhance the BP stability, fuel/air distribution and current collection in electrodes and electrolytes [29], [30]. Several aspects of graphene-based materials such as catalytic and electrochemical characteristics have been thoroughly examined [31], [32]. Most of the recent evaluations concentrated on a particular application area linked to the working principles of e-fuels such as ORR [21], fuel oxidation [33], [34], membranes [35] and BPs [36]. Typical examples of e-fuel fabrication paths are shown in Fig. 1.

E-fuels serve as a bridge between the power and other areas such as industries, transportation, energy and pollution management. Renewable electricity have prompted e-fuels made from non-fossil CO_2 which have the potential to complement other alternative fuels with significant climate benefits worldwide. The purpose of this review was to assess the benefits of adding graphene oxide to e-fuels towards making them more efficient in energy delivery compared to other fuel sources by improving their overall performance.

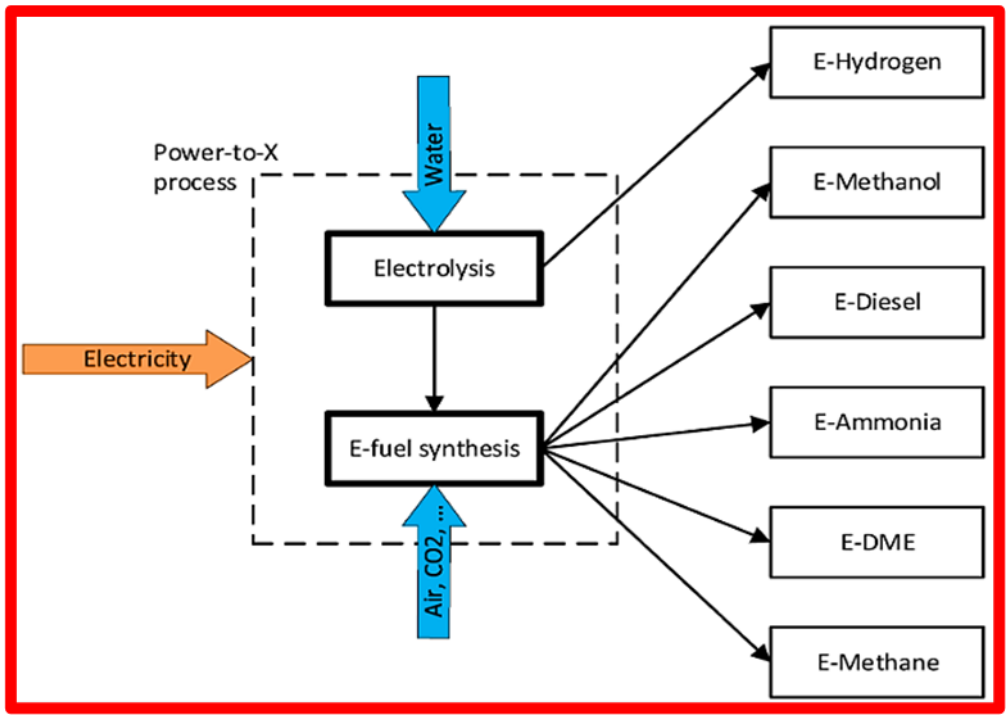

Fig. 1. E-fuel fabrication paths (derived with permission from [37]).

2 Fabrication of E-Fuels

To create various energy carriers, such as e-fuels, hydrogen and carbon dioxide are fed into a synthesis reactor [38]. The most prevalent energy carriers include methanol, diesel, ammonia and methane [39]. Methane and methanol are examples of small molecules that appear to be desirable since they do not require as many stages in the processing as ethanol, which result in efficiency losses [40]. As fuel is created, high quality oxygen and heat are also formed in the course of fabrication using electricity. Heat is produced at both high and low temperatures in the fuel creation vessel and electrolysis individually [41]. For instance, the heat can be produced in a cooking appliance and the oxygen can be used in hospitals or in industrial processes. Currently, using natural gas for steam reformation is the most popular method of producing hydrogen. Using a more energy-intensive technique of producing hydrogen, such as water electrolysis, is a less popular approach [42]. A significant amount of energy is required to manufacture large amounts of hydrogen, and as hydrogen is a renewable fuel, it is preferred that the energy originate from renewable sources [43].

Electrolysis can be classified into three primary types: solid oxide, alkaline and proton exchange membrane (PEM) [43]. Most current electrolyses are made to operate at steady state under a constant load. However, a flexible manufacturing process such as quick ramp times and low electrolyser start-up costs is required to control harmonising electrofuels, or to be able to follow non-dispatchable renewable power foundations [44]. Fig. 2 presents various e-fuel fabrication paths.

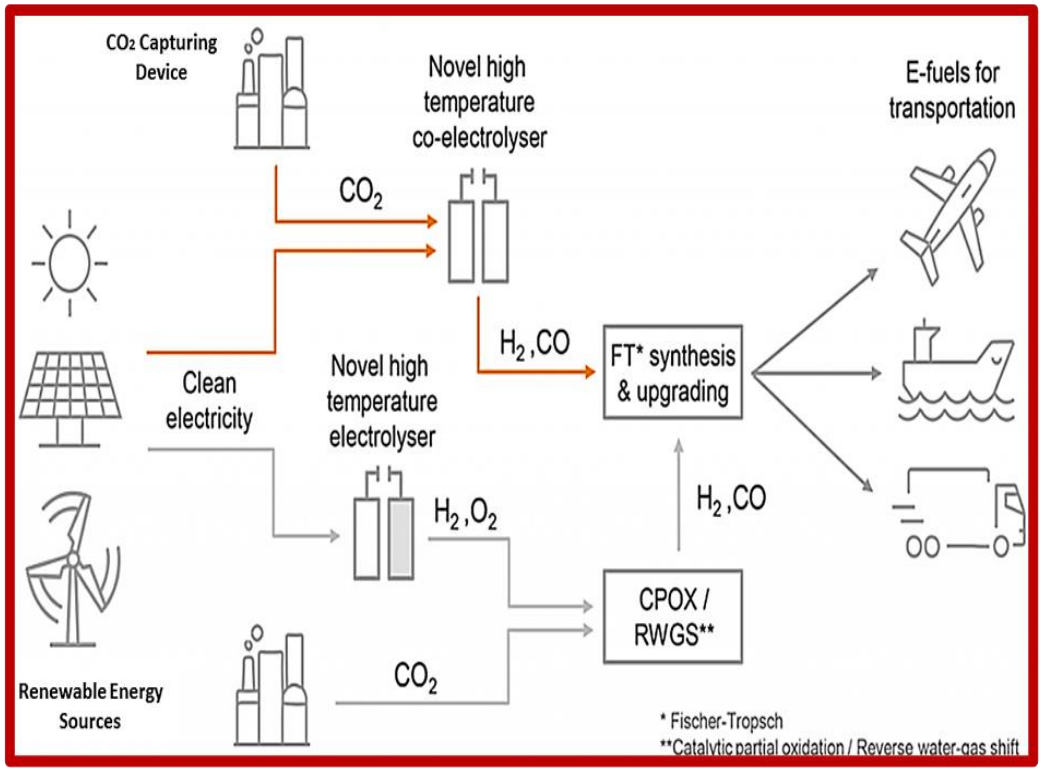

Fig. 2. Various production routes of e-fuels (copied with permission from [45]).

The excess CO_2 can originate from various processes such as those from biofuel, natural gas, flue, fossil fuels, biomass, industries or companies, oil refineries, geothermal energy and air (Fig. 3). Significant volumes of CO_2 are produced as a by-product in the manufacture of biofuels, such as through the fermentation of sugar to ethanol, the anaerobic digestion of domestic wastes to biogas or the gasification of biomass to methane [46]. Gases from ammonia and biofuel facilities have extremely high CO_2 concentrations. According to Mohseni [40], if a synthesis reactor is used, the amount of methane produced from the digestion or gasification of biomass can rise by 44–136%, allowing the emitted CO_2 to react with additional hydrogen. Reiter and Lindorfer [47] reported that the major sources of CO_2 radiations in Austria comes from iron, steel and cement industries. To create a fuel that is climatic neutral, the CO_2 must come from a

non-fossil source. In Austria, the generation of bioethanol and upgrading of biogas accounted for a minor portion of CO_2 emissions.

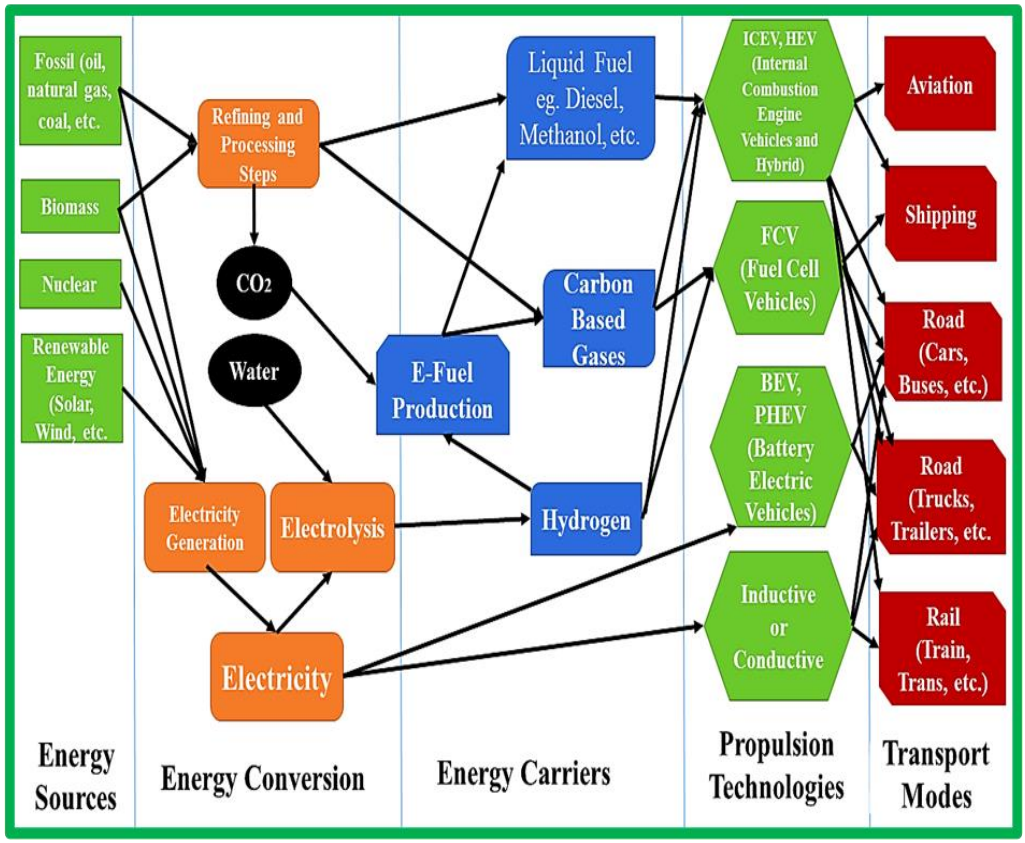

Fig. 3. Distinct energy sources, energy conversion technologies and energy carriers of e-fuels.

2.1 CO_2 for E-Fuel Production

Carbon (II) oxide (CO_2) can be captured from various sources by re-combustion, post-combustion or oxy-combustion [48]. The exhaust stream of a bioethanol plant has a high concentration of CO_2, therefore no additional energy or purification step is required during the capture process. Methane, CO_2 (40%) and a few trace elements are contained in biogas generated, for instance, from the fermentation of household trash. However, a cleaning procedure to remove the CO_2 is required to improve the biogas to fuel quality. Numerous industries and energy technologies, such as those that produce steel and iron, ammonia, cement, refineries, fossil fuels and biomass combustion, need CO_2 refinement after capturing [49], [50]. Fig. 4 is a representation of a CO_2 electrolyser illustrating devices that display semi-reactions at various electrodes.

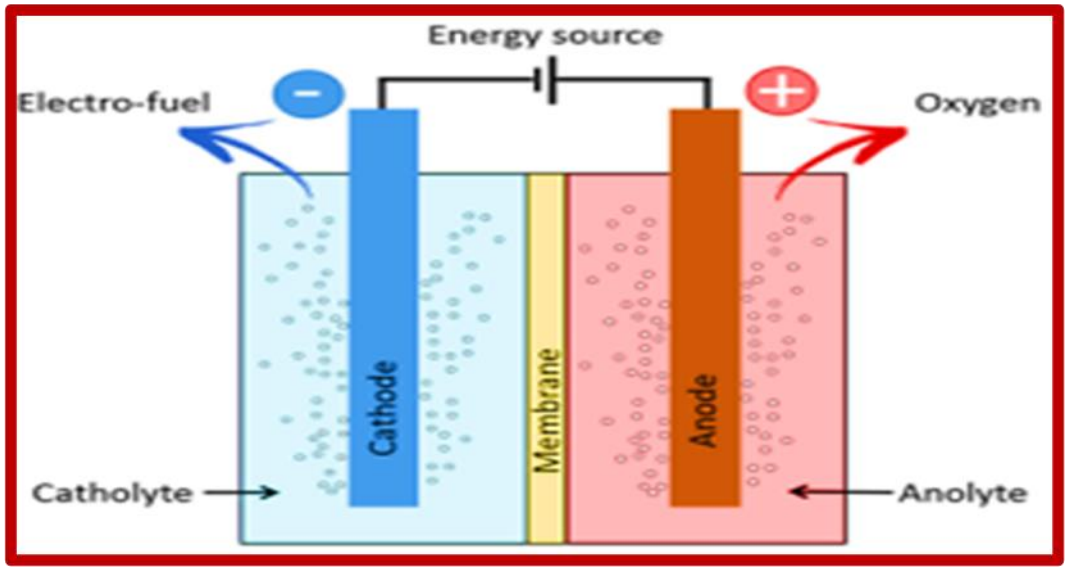

Fig. 4. CO_2 electrolyser illustrating devices that show semi-reactions (adapted with permission from [50]).

The amount of CO_2 in the air is about 400 parts per million, and extracting it from the atmosphere would take two to four times as much energy as extracting it from flue gasses. Strong bases that may efficiently remove CO_2 from the environment include NaOH, KOH and $Ca(OH)_2$ [51], however, the process of regenerating the bases uses a lot of energy, and efforts are being made to create alternate materials that may use less energy. Many designs are technically possible, and various methods and materials have been suggested but are in a premature phase of growth. Additional studies and pilot plants are required to maximise the technology. Fig. 5 displays the CO_2 capturing techniques.

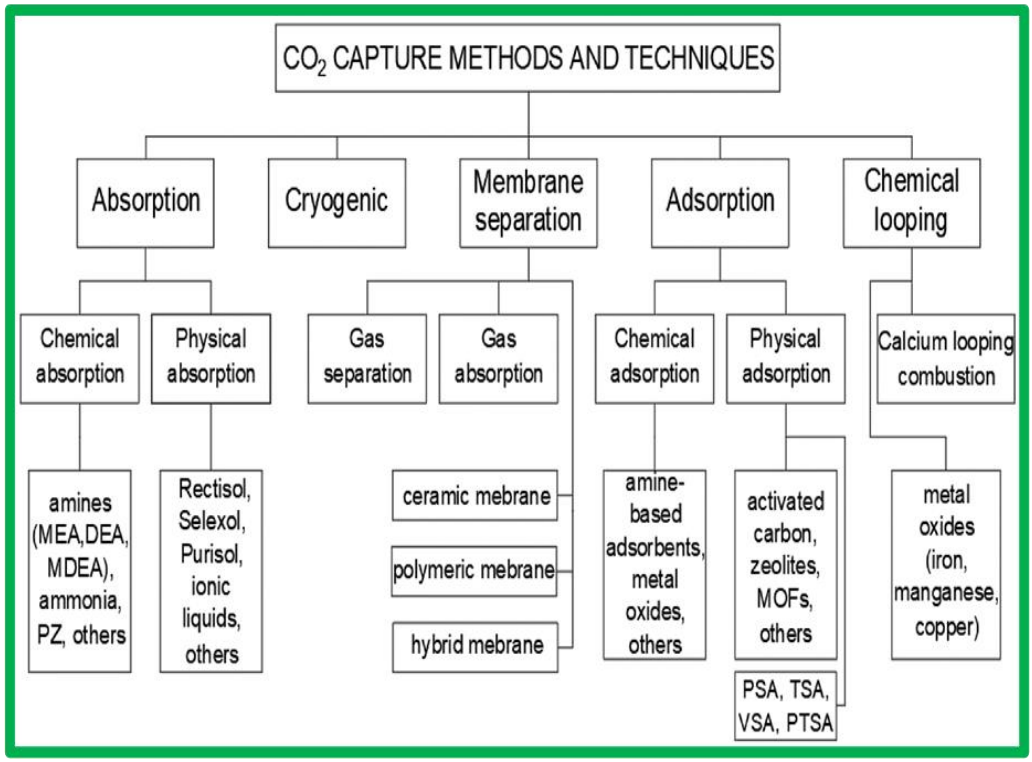

Fig. 5. CO_2 capturing methods (copied with permission from [48]).

2.2 Hydrogen for E-Fuel Production

By employing an electric current to separate hydrogen from water, a process known as electrolysis generates green hydrogen. This procedure is environmentally friendly because the electricity it uses comes from renewable sources such as solar and wind power. About 30% of the energy used in the process of creating green hydrogen is lost during energy conversion, which means that 70% of the energy used is locked up in hydrogen. The current most popular method for producing hydrogen is using natural gas to create steam through restructuring. Using a more energy-intensive technique of producing hydrogen, such as water electrolysis, is a less popular approach. A significant amount of energy is required to manufacture large amounts of hydrogen, and as hydrogen is a renewable fuel, it is preferred that the energy originate from renewable sources. Electrolysis can be classified as three primary types: solid oxide, alkaline and PEM. Most current electrolysers are made to operate at fixed state under a continuous load. Nevertheless, the production process must be flexible for e-fuels to be power corresponding, or capable of following a non-dispatchable renewable power source.

2.3 Fischer-Tropsch Synthesis of E-Fuels

E-fuels, referred to as artificial (synthetic) fuels or electrofuels, are hydrocarbon fuels (such as diesel, methanol and methane) made primarily from water and CO_2 streams, with electricity serving as the energy source. The Fischer-Tropsch synthesis (FTS) is typically employed in the invention of various fuels, including e-fuels. The two scientists, Franz Fischer and Hans Tropsch, created the synthesis method known as the FTS technique. Researchers have been interested in this approach in recent decades since it was argued that producing liquid hydrocarbons using this promising clean technology could be a viable alternative to address the lack of liquid transport fuels. Syn-gas (H_2 and CO) is converted into synthetic liquid fuels and valuable compounds using the FTS technology. This synthesis is a surface polymerisation reaction, which means that the hydrogen and carbon monoxide reagents react on the catalyst's surface as it happens. Fig. 6 provides a visual representation of how it operates.

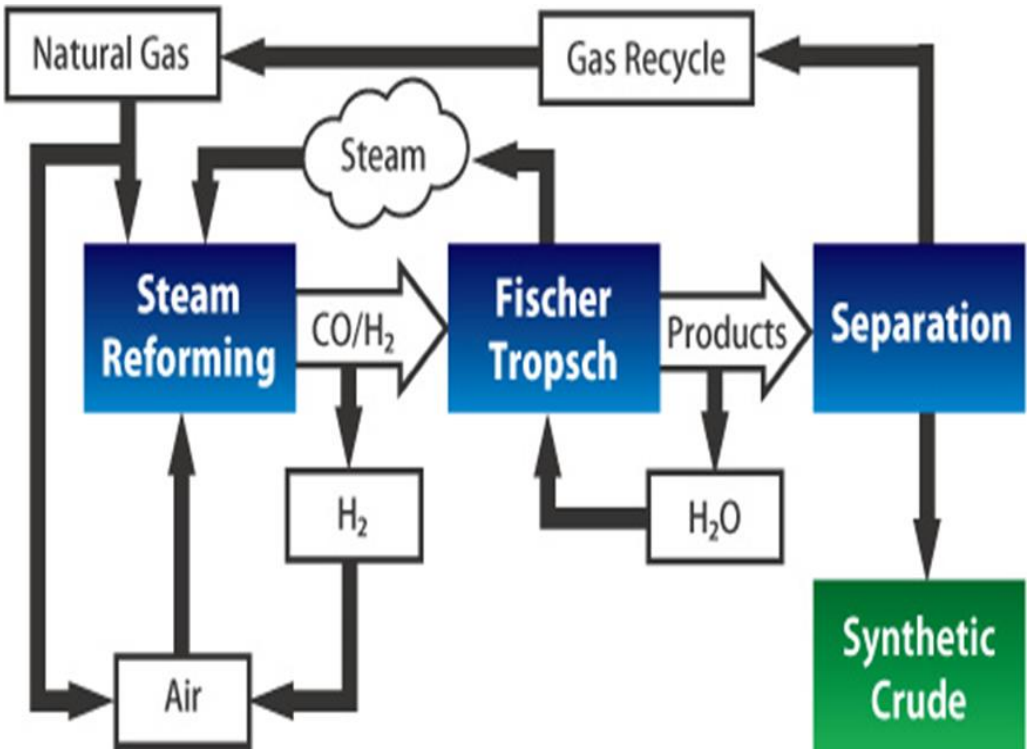

Fig. 6. Working mechanism of Fischer-Tropsch synthesis of e-fuels (copied with permission from [52]).

2.4 Graphene

In recent years, owing to its exceptional qualities including its zero energy band gap, exceptional electrons flexibility in room temperature, higher thermal conductivities, stability, massive superficial areas and impenetrability to gases, graphene is currently the topic of all-encompassing enquiry globally [53]. The graphene charge carrier travels little micrometres at room temperature still maintaining its configuration (shape or structure) and exhibiting core mobility. In the domains of energy storage, electronics, chemical sensors, optoelectronics, nanocomposites and health (for example, osteogenic materials), more scientists are becoming aware of graphene-based materials. Graphene, which consists of a solitary sheet of carbon atoms, is one of the isotopes of carbon. The arrangement of these carbon atoms forms a two-dimensional honeycomb lattice structure. The carbon–carbon bond distance in a single graphene sheet is approximately 0.142 nm [54]. The minimal mass of the particles in graphene, which results in the inconsistent quantum Hall effect and the absence of localization, is one of its distinguishing and essential characteristics that attracted attention from researchers. [55]. Graphene-based materials enjoy numerous applications in energy storage devices such as supercapacitors and lithium-ion batteries [56], gas detection [57] and conducting electrodes [58]. The remarkable pace of growth in recent times for graphene consciousness suggests that graphene is a promising new material that scientists are searching for to advance the fields of science, engineering, health and composites formation. When graphene is added to a composite, active material is created at the nanoscale, which improves non-faradaic capacitive behaviour, and conducts and prevents disintegration [59].

Graphene generates a bodily obstacle amid the active material and the electrolyte, refining rate capability, specific capacitance and cycling stability [2]. The theoretical surface area of graphene is 2 630 m^2/g, almost two orders of magnitude greater than graphite powder, which has a surface area of 10 m^2/g [60]. Graphene's strong interactions with π electrons prompts great adsorption capacity to the reactants, which allow them to be used as catalysts or catalytic supports. Graphene valence and conductance bands overlap, which result in zero band gap semiconductor with great carrier mobility (~10 000 cm_2/Vs at relativistic speed ~106 m/s) [61]. Since graphene's nobilities are less affected by temperature, ambient temperature can be used to obtain an ultrahigh mobility rate. The transfer of electronic density among the graphene systems and nanostructures are more favourable owing to its distinct electrical characteristics [59]. A unique electrical structure is displayed by the perverted bilayer graphene in conjunction of magic angles, where the Fermi velocity vanishes at the Dirac point [62]. The applications requiring rigorous heat management and the reactions displaying great endothermicity or exothermicity benefit from graphene's decent thermal conductivity (~5 000 W/mK for a mechanically exfoliated monolayer graphene) [63]. The higher density of electroactive locations at graphene's edges contributes to the material's quick heterogeneous electrons transfer (HET) rates, which is higher at graphene's edge planes than it is at basal or defect-free planes [64], [65]. Some of the properties of graphene-based materials are shown in Fig. 7.

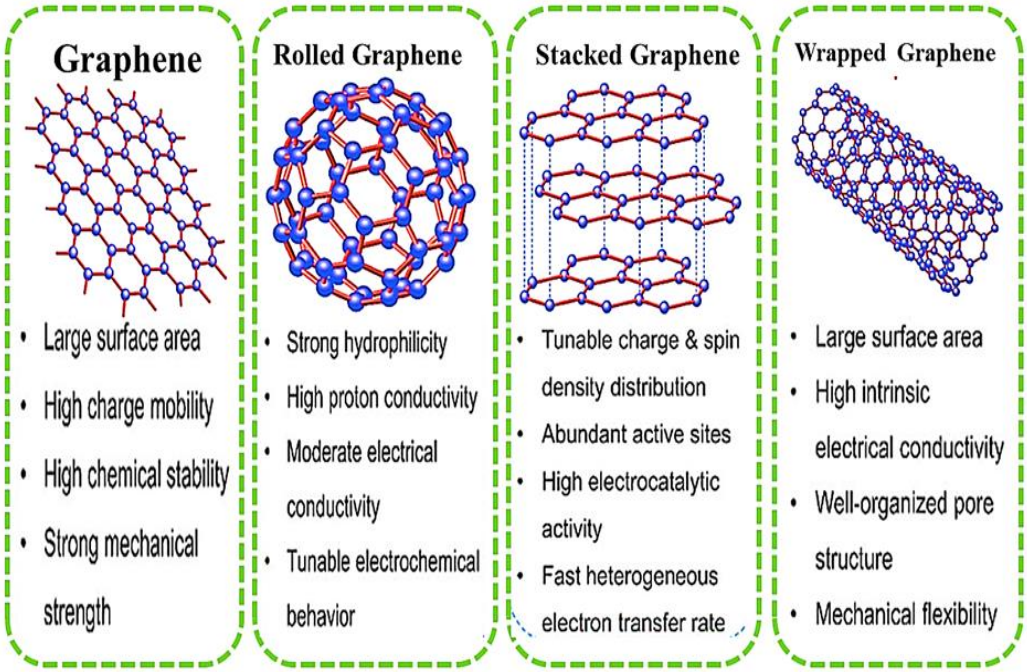

Fig. 7. Properties of graphene materials.

2.5 Synthesis of Graphene

Any technique of generating or producing graphene from graphite is known as graphene production or synthesis. The required mass and pureness decides which approach should be used during the synthesis [66]. The properties and performance of the generated graphene are determined by the production procedure. By employing Scotch tape and a method known as micro-mechanical cleavage, the first graphene was created by removing monolayer sheets from three-dimensional graphite [11]. The bottom-up approach and the top-down method are the two main categories for classifying a large range of synthesis methods. The primary techniques used in the bottom-up approach include arc discharge, chemical vapour depositions (CVD) on catalytically energetic metal and epitaxial development within distinct crystal [11], [67]. The top-down technique comprises liquid-phase exfoliation, chemical exfoliation, ball milling, ultrasonic treatment, electrochemical exfoliation, and high-shear mixing [24], [67]. Graphene sheets emanate from a single stratum, and double and multiple strata, and they are employed in a ranges of science and technology domains, including energy storage devices, biology, memory, electronics and sensors [68].

3 Graphene-Based Materials for E-Fuel Applications

Graphene materials have been shown to offer many benefits when used as active ingredients in e-fuels. The prospective usage of graphene derivatives as electrocatalysts for ORR and fuel oxidation seems promising because they possess major surface area and highly conductive qualities [69]. The graphene-coated polymer membranes have minimal fuel permeability, good tensile strength, and high ionic conductivity. The conductivity and resistance to corrosion of BPs can both be improved with graphene.

3.1 Graphene in Oxygen Reduction Reactions and Electrocatalysts

Typically, metal nanoparticles are supported by conductive graphene-based material to help transmit electrons to the electrode surfaces. For instance, it was discovered that N-doped graphene support increased nucleation and development kinetics of nanoparticles and backing/catalysts in chemical interaction, consequently enhancing the distribution and permanency of Pt-Co alloy nanoparticles [70]. The proton-exchange membrane fuel cells (PEMFC) using a Pt-Co/N-doped graphene cathode validated a supreme power density of 805 mW/cm^2 at 60 °C, which was four times greater than the PEMFC using a commercial Pt/C cathode. Catalysts free of platinum groups in metals (PGM) are showing more promise for widespread commercialisation [70].

According to Liang *et al*. [71], the Co_3O_4/rGO composite has better stability (less decrease in ORR activity over 25 000 seconds) compared to the Pt alkaline bath, but it also exhibits comparable catalytic activities with an ORR onset potential (Eonset) of approximately 0.83 V compared to reversible hydrogen electrodes (RHE). Its exceptional activity was ascribed to the metal oxide and graphene's synergistic chemical coupling effects. Big superficial area and penetrability, superior electrical conductivities and connected pores architectures of 3D graphene not only increase the number of anchor sites for immobilising metal oxides nanoparticles, which enhances reactants mass transit [72], [73].

It was discovered that, in Pt-Fe/HSG electrode using improved surface fluids approach and 3D honeycomb-designed graphene (HDG) for ORR, $Pt40Fe_{60}$/HSG demonstrated extraordinary mass activities of 1.70 A/mgPt, 14.2 times greater compared to marketable Pt/C's 0.12 A/mgPt. In addition, melamine formaldehyde resin was used as a lenient prototype and source of nitrogen to prepare Fe/N/S integrated Fe_3O_4 nanoparticles on 3D HSG (Fe_3O_4/FeNSG-3) as PGM-free ORR catalyst [74], [75], [76]. Defective and heteroatom-doped graphene can serve as perfect supports for securing lone metal atoms [77]. This solitary atom catalyst (SAC) supported by graphene demonstrated strong ORR activities and selectivity for the four electrons reactions pathway, along with long-term stability in either acidic or alkaline environments. The durable connections among various atoms and graphene derivatives provides the large density of active sites and higher charges redistributions, hence better performances [78].

3.2 Graphene-Free Metal ORR Electrocatalysts

Metallic leaching and metal ions pollution problems brought on by metal-based catalysts can be resolved by graphene-based free metal catalysts [79]. N-doped graphene was investigated by Qu *et al*. [80] as a non-metallic electrocatalyst for ORR. Using the CVD method, they produced N-doped graphene with a ratio of about 4% N/C, which demonstrated a threefold increase in constant catalytic current density compared to marketable Pt/C electrode in 0.1 mol/L KOH. Ultrathin N-doped perforated carbon layers on GNS were described by Sun *et al*. [81], and in 0.5 mol/L H_2SO_4 it demonstrated good ORR performances (Eonset = 0.80 V compared. RHE; E1/2 = 0.65 V vs. RHE).

Extensive attempts were undertaken to comprehend the ORR activity-related catalytic processes and active regions of N-doped graphene [82]. Founded on a matched relationship between activity and graphitic N contents, the increased ORR activity of N-doped graphene was credited by Geng *et al*. [83] to graphitic N. Both graphitic and pyridinic nitrogen were shown to be active sites for ORR, according to Lai *et al*. [84]. To be more precise, the pyridinic N raised the ORR onset potential whereas the graphitic N defined the restraining current density. It was shown that in alkaline conditions, pyridinic-N-rich graphene exhibited selectivity towards the ORR four-electron pathway [85]. Guo *et al*. [86] recently discovered that the electron scarce carbon combines with pyridinic nitrogen in N-doped graphene and performs well in the ORR activity.

The oxygen/hydroxyl (O-OH) bond is broken by two protons in the four-electron route, which results in adsorbed OH and a proton-OH species reaction that form H_2O. It is also feasible to use the two-step, two-electron pathway, in which one proton and adsorbed OOH species react to produce H_2O_2 before it is reduced to H_2O [87]. To boost graphene's ORR activity, additional often-employed dopants include phosphorus, boron and sulfur. In graphene-free metal ORR, the graphitic planes' electro neutrality broken, S-doped graphene outperformed commercial Pt/C in alkaline conditions with regard to ORR catalytic activity [88]. Multi-doped graphene materials, as N, P co-doped graphene [89], can achieve excellent ORR activity. Quaternary graphene can be doped with B, N, P and S [90]; tri-doped graphene with B, N and P [91]; and tri-doped graphene with F, N and P [52]. When the correct two elements are co-doped, the energy gap can be closed and chemical reactivity and conductivity can be increased [92]. The redistribution of spin and charges concentrations caused by the double dopants amplified the number of energetic spots for ORR [92] and electrochemical reactions [93].

3.3 Graphene Metal-Based ORR Electrocatalysts

The noble metal's dispersion can be enhanced and charge mobility in fuel oxidation facilitated by graphene-based materials' vast superficial area, higher electrical conductivities and customisable fastening positions. The rate of oxygen evolution reactions (OER), ORRs and hydrogen evolution reactions (HER) within the electrode control the efficiency e-fuels [94]. The overall e-fuel efficiency is reduced because of

these processes, which happen much more slowly. The most often used electrocatalysts to speed up processes are metals and metal oxides including Pt, RuO_2 and IrO_2 [16], [76]. Despite the encouraging outcomes, the widespread use of these electrocatalysts is constrained by a number of factors, such as their exorbitant cost, RuO_2 oxidation, Pt CO poisoning, and scarcity [95]. The development of effective graphene-supported electrocatalysts for the formic acid oxidation reaction (FAOR), ethanol oxidation reaction (EOR), and methanol oxidation reaction (MOR) has attracted numerous interests triggered by their fast charge transference rates and biocompatibilities; graphene-based materials show great promise as anodes for microbial fuel cells (MFCs) [71].

Because of its special qualities and relatively cheaper cost, graphene or its derivatives are a great substitute for these traditional electrocatalysts. Since graphene has a zero band gap, it has little catalytic activity [96]. However, doping graphene with different heteroatoms changes its electronic characteristics, creates more vigorous spots and greatly boosts its electrocatalytic activities. The various electrocatalytic reactions in e-fuels can be strongly influenced by the shape of an electrocatalyst based on graphene.

3.4 Graphene-Based Polymer Membranes

To improve the ionic conductivities and gas impermeabilities of polymer membranes, graphene and its derivatives are frequently employed as decorations. In comparison to conventional polymer membranes, the composites membranes have stronger ionic conductivities, lesser fuel gas permeability, greater mechanical and chemical stability, all of which enhance fuel cell longevity and performance. An essential component of the e-fuel system is polymer electrolyte membranes (PEMs) [9]. Nafion, Flemion and Aciplex are examples of PEMs that are used commercially and are mostly centred on perflurosulfonic acid (PFSA). However, they exhibit encouraging outcomes, their broad use is limited by various circumstances [97]. The most frequent PEMs-related challenges are high operating temperatures and high rates of performance in extremely humid environments, fuel crossover problems, high costs, essential synthesis methods and water balancing problems [5], [97], [98]. A key goal of e-fuels technology is now to build a PEM with sufficient conductivity that can operate in high temperatures and low humidity environments [20].

By increasing the reaction rate, graphene impregnation in PEMs improves e-fuel devices durability and efficiency [9], [76]. Because of its enormous electrical conductivity, higher charge carrier degrees, wide superficial area, and cheaper fabrication cost, graphene and its 2D variants are lucrative to use [34]. Higher proton permeability, increased thermal and electrochemical stability, high rates of water absorption, low permeability to reactant species, higher mechanical stability and reduced cost are all requirements for a PEM [5].

3.5 Bipolar Plates of Graphene-Based E-Fuels

A BP is a crucial component of e-fuel devices. Its duties include supporting the cell, distributing oxidant and fuel to the electrode surfaces and gathering current for the cells. It should therefore have low gas permeability, strong mechanical properties and high electrical conductivity [15], [99]. BPs in e-fuel devices are made of both metals and non-metals. Graphene-based materials are highly significant resources attracting interest from researchers who study BPs because of their high electrical conductivity (106 S/cm), low specific gravity, and high resistance to corrosion [22], [76].

Graphene-based BPs, however, are weak mechanically. By using them to create a BP out of a composite of metals, this can be avoided. Although metallic plates are strong and have good electrical conductivity, they are susceptible to corrosion [36]. However, as regards metal and non-metal BPs, scientists discovered a notable increase in the outcomes by adding graphene as an auxiliary resource in BPs [15].

In e-fuel devices, BPs are used for mechanical support, gas and heat distribution, and current collection. BPs are designed to provide high mechanical strength, low permeability to gases, low interfacial contact resistance, high electrical and thermal conductivities, higher corrosion resistance and are lightweight. [36]. Because of its strong conductivity (103 S/cm) and good corrosion resistance, graphite is the most popular resource for BPs used in e-fuel devices. However, the expense of production and its low mechanical strength make graphite less practical for use in these applications [29], [36].

To create highly conductive polymeric BPs, graphene derivatives can also be used as fillers [25]. The electrical conductivity of fillers was increased to 114 S/cm by adding 20 weight per cent carbon black [25]. The highly filled graphene/polybenzoxazine composites prepared by Plengudomkit *et al*. [100] had a 60 weight per cent graphene content and demonstrated high flexural modulus (18 GPa), flexural strength (42 MPa), electrical conductivity (357 S/cm), thermal conductivity (8.0 W/mK), and little water immersion (0.06% at 24 hours absorption). A GO/polypyrrole composite was created by Jiang *et al*. [101] and then coated on stainless steel using an in-situ electrodeposition technique. The interfacial union among metallic and polymers was improved and the penetration of corrosive classes was inhibited by the existence of GO inside composites BP. However, difficulties in using materials based on graphene in BPs still exist. In galvanic corrosion mechanisms or the interaction amid ion or defect/grains margins in graphene, it was discovered that graphene did not increase corrosion resistance for stainless steel plate in absence of metal coatings or at high temperatures (> 60 °C) [102] [103]. It is possible that interfacial contact resistance will rise owing to the comparatively low electrical conductivity of GO or rGO coatings. In addition, hydrophobic graphene is difficult to adhere to metal plate in the absence of the need for a binder [36]. It would be inevitable for the cost and interfacial contact resistance to increase with the addition of a binder.

Another challenge is to designate channels for gas flow within the graphene lattice without sacrificing its electrical and corrosion resistance [36]. The review compiled several studies on applications of based materials in e-fuel applications to enhance performances. Table I presents the summary of the performance and applications of graphene-based materials in e-fuels.

TABLE I
SUMMARY OF THE PERFORMANCE AND APPLICATIONS OF GRAPHENE-BASED MATERIALS IN E-FUELS

S/N	Graphene-Based Material	Application	Mechanisms	Performance	Ref.
1	Graphene doped Ni foam	Bipolar plates	Graphene's excellent conductivity makes it an effective corrosion barrier in e-fuel devices.	Corrosion is reduced by half with an optimum power density of 967 mW/cm^2	[104]
2	Graphene-doped Nafion membranes for DMFC	Bipolar plates	Methanol is given twistiness by graphene, which does not change the proton conductivity.	E-methanol permeability of 2.19×10^{-6} cm^2/s with supreme power density of 75 mW/cm^2 at 70 °C	[75]
3	GO peels for H_2/O_2 e-fuels	Electrolytes	Great proton transference and H_2 and O_2 gas impenetrability	High proton conductivity up to 10^{-6} to 10^{-4} S/cm at an ultimate power density of 13 mW/cm^2 at 25 °C	[105]
4	Composites of rGO@Polyacrylamide@Graphite brush	Anode in MFCs	Huge surface areas, great electrons conductance and high affinity for microbial biofilms	Activation polarisation resistance of 4.4 Ω/cm^2 within the device and a supreme power density of 782 mW m−	[106]
5	PtPd-doped rGO	EOR	Synergistic effects among Pt and Pd with enhanced ligands	Greater catalytic activities compared to metallic Pt or Pd catalyst	[107]

S/N	Graphene-Based Material	Application	Mechanisms	Performance	Ref.
6	Composites of PtRh nanowires and graphene nanosheets	EOR		Higher mass fold activities equated to Pt/C	[108]
7	Pt-doped graphene nanosheet	MOR	Variation in the electronic structures of Pt constellations	E-fuels advanced activities and more CO acceptance	[109]
8	Edge-sulphurised graphene	ORR	Doped sulphur atoms and sulphur oxides at graphene edges proliferate spins and charges density	Higher ORR electrocatalytic activities, improved e-fuel fussiness and lengthier stability	[110]
9	Co_3O_4@N-doped graphene	ORR	Enhanced synergetic chemical combinational properties among Co_3O_4 and in graphene	Enhanced catalytic activities and bigger stability	[71]
10	Co_3O_4/N-rGO	Electrocatalyst	It possesses high ORR activities	Little cost catalyst higher durability	[71]
11	Ru@N/G@750	Electrocatalyst	The ORR activities are 7.5 times higher	Excellent durability and onset potential between 0.89 and 0.75 V	[111]

4 Review of the Types of E-Fuel

Carbon-derived fuels such as methanol or methane, which are created with electricity serving as the main energy source, are collectively referred to as “e-fuels” or “electrofuels”. CO_2 is the fuel’s source of carbon and can be recovered from a variety of industrial operations, such as waste, exhaust gases, the sea and the air. E-fuel fabrication remains in its early stages, and numerous obstacles must be removed before e-fuels are widely distributed, accepted and used. E-fuels can also be classified with respect to their state and carbon content as presented in table II [112].

TABLE II
STATE AND CARBON CONTENT CLASSIFICATION OF E-FUELS (ELECTROFUELS)

S/N	Liquid	Gas	Low Carbon
1	E-hydrogen	E-methanol	E-methane
2	E-methane	E-diesel	E-methanol
3	E-ammonia		E-diesel
4	E-DME		
5	E-kerosene		

4.1 E-Hydrogen

The electrolysis of H_2O is an electrochemical practice that uses electricity to break down H_2O into oxygen and hydrogen, which produces e-hydrogen. Power-to-hydrogen (PtH_2) presents a procedure for producing hydrogen by employing electrolysis using a renewable energy source. In the case of power produced by a renewable energy source, electrolysis is a crucial step in the production of sustainable hydrogen. Although this method is well known and devoid of greenhouse gases, it only produces only 4% of the hydrogen produced overall. Applying electrical energy to split water into hydrogen and oxygen (equation 1) is recognis0ed as water electrolysis. The following lists the electrochemical reactions that take place at the electrodes of an alkaline electrolyser (AEC) [113]:

- the positively charged anode is the site of the oxidation reaction (equation 2); and
- the negatively charged electrode (cathode) is the site of the reduction reaction (equation 3).

$$\text{Overall: } H_2O\,(l) \rightarrow H_2(g) + \frac{1}{2}O_2(g)\ \Delta Hr = 285.83\ \text{kJ/mol} \quad (1)$$

$$\text{Cathode: } 2H_2O(l) + 2e^- \rightarrow 2OH^- + H_2(g) \quad (2)$$

$$\text{Anode: } 2OH^- \rightarrow H_2O\,(l) + 2e^- + \frac{1}{2}O_2(g) \quad (3)$$

AECs, proton exchange membrane electrolysers (PEMEL) and increased temperature solid oxide electrolysers (SOE) are the three different types of water electrolyser. The primary features of the three electrolysers are shown in Table III, with additional parameters listed in [114], [115], [116], [117]. The most developed commercially accessible technology, known as AEC, has been applied extensively in the chemical industry and in the large-scale synthesis of hydrogen. It typically functions between 60 and 80 °C and consists of two electrodes submerged in an aqueous electrolytes [112]. AECs can operate at atmospheric pressure (atmospheric AEC) or high pressure (pressurised AEC) [114]. Pressurised AEC has the benefit of producing compressed

hydrogen, which can be used straight into grids or in other applications without first having to be compressed. This means that less energy is consumed because no additional energy is needed [40].

TABLE III
FEATURES OF THE THREE TYPES OF ELECTROLYSER

S/N	Type of Electrolyser/Property	Alkaline	PEMEL	SOE
1	Technology development	Profitable [114]	Marketable [114]	R & D/Laboratory [114], [115]
2	Working temperature (ºC)	60–80 [115]	50–80 [115], [117]	600–1 000 [112], [118]
3	Pressure (bar)	< 30 [114]	< 30 [114]	< 30 [114]
4	Energy consumption (kWh/m^3H_2)	4.5–7.0 [114]	4.5–7.5 [114]	2.5–3.5 [114]
5	Cell voltage (V)	1.8–2.4 [114], [116]	1.8–2.2 [114], [116]	0.95–1.3 [114], [116] 0.7–1.5 [115]
6	Voltage efficiency (%)	Low efficiency [43] 62–82 [114], [116]	Moderate efficiency [115] 67–82 [114], [116]	Higher efficiency [115] 81–86 [114], [116]
7	Lifespan (year)	15–30 [119] 20–30 [114], [116]	10–20 [114], [116], [119]	Nil
8	H_2 fabrication rate (m^3/hr)	< 760 [114], [116]	Approximately ~ 450 [117] < 30 [116]	Nil
9	Hydrogen purity (%)	> 99.8 [115]	99.999 [115]	Nil

4.2 E-Methanol

Nowadays, fossil fuels account for nearly all of the production of methanol. Fig. 8 shows the e-fuel fabrication processes. Methanol (CH_3OH) is among the prominent fuels produced from power-to-liquid (PtL) technology. Methyl tertbutyl ether (MTBE), formaldehyde, dimethyl ether (DME), acetic acid and numerous goods including paint, plastic, house supplies and auto components are among the valuable feedstock that are produced using methanol [120]. In addition, it is regarded as a clean synthetic fuel and a great solvent that can be used in power generation, wastewater treatment, industrial boilers, transportation and cooking. It may also be used as a hydrogen carrier for fuel cells and as an alternative source of chemical energy [121], [122]. Methanol is easily handled, transported and distributed in a liquid state under typical ambient circumstances [122]. Currently, 98 million tons (Mt) of methanol are produced worldwide each year from fossil fuels (coal or natural gas). Methanol produced 0.3 gigatons (Gt) of CO_2 yearly, approximately 10% of all discharges from chemical industries. If businesses continue to depend on only fossil fuels, the demand for methanol is predicted to rise to 500 Mt by 2050, which would result in the annual release of 1.5 Gt of CO_2 [121]. It is therefore critical to address methanol production emissions

and develop alternate processes for renewable methanol production to decarbonise the chemical industry. The following reaction equation 4 [1] is the catalytic hydrogenative transformation of CO_2 to methanol, which produces methanol:

Overall: CO_2 (g) + $3H_2$ (g) → CH_3OH(l) + H_2O (l) $\Delta Hr = -49{:}2$ kJ/mol (4)

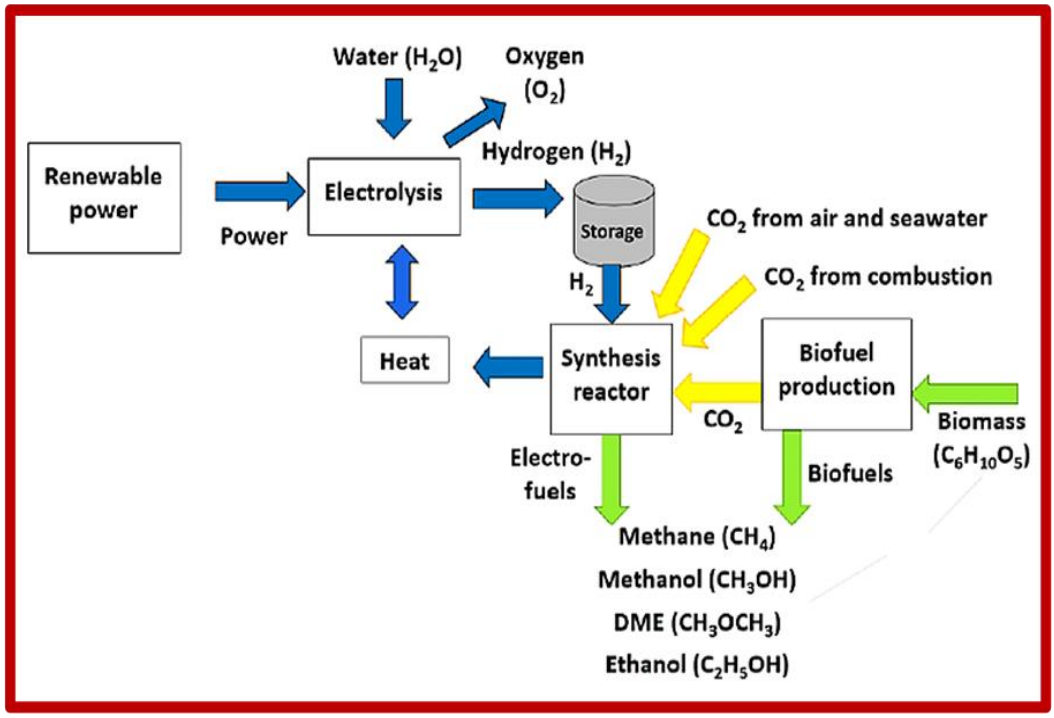

Fig. 8. The e-fuel production processes (copied with permission from [123]).

The catalyst based on copper/zinc oxide facilitates an exothermic catalytic reaction with a 3:1 ratio for H_2:CO_2 that can occur in a range of temperatures and pressures between 200 and 300 °C and 50 to 100 bar, respectively [124]. A variability of carbonaceous sources such as natural gas, coal, biomass byproducts and CO_2 extracted from industrialised chimney smokes or directly from the air can be used to produce methanol [125]. It is obvious that most of the methanol fabrication processes still rely on fossil fuels, with coal accounting for the remaining 65% and natural gas for approximately 65%. Renewably produced methanol makes up a minor portion of the total, at 0.2% [125]. Methanol can be characterised by lower or higher carbon contents centred on the type of feedstock used, the conversion process, and the emissions that are produced. Methanol generated using syngas by coal gasification or natural gas remodelling (brown and grey methanol), which is regarded as having a high carbon intensity. It has been

noted that, because natural gas has high hydrogen/carbon ratios and few impurities, it produces less emissions when used to create methanol than when coal is gasified [125].

However, methanol (blue and green methanol) derived from renewable resources is regarded as having a low carbon intensity. For a system to be deemed entirely renewable, all of its feedstocks must come from solar, wind, hydro or geothermal energy. Either the bio-methanol or the e-methanol method can be used to manufacture renewable methanol, also known as green methanol. Bio-methanol is produced through gasification of biomass feedstocks, including paper, sewage, wood, agricultural waste, and biogas from landfills. Green hydrogen, which is generated from renewable electricity, and collected CO_2 are combined to form e-methanol. The CO_2 that has been caught can also be categorised as renewable CO_2 and comes from biomass and direct air capture (DAC), though non-renewable CO_2 is reprocessed from power plants and companies that rely on fossil fuels [14]. Blue methanol is created by adding blue hydrogen to the methanol synthesis, which is another method of lowering CO_2 emissions. By combining grey hydrogen with carbon capture and storage (CCS) assistance, blue hydrogen is created from natural gas through the processes of auto thermal reforming (ATR) and steam methane reforming (SMR) [126]. This combination, along with other combinations of various methanol "colours", makes it easier to produce sustainable green methanol while reducing process-related greenhouse gas emissions.

4.3 E-Diesel

In the past, as an alternative to conventional fossil fuels, syngas (CO/H_2) was converted to liquid hydrocarbons using the Fischer-Tropsch (FT) process. The FT could be linked to biomass and also coal gasification and natural gas (NG) restructuring [50]. Equation 5 shows the reactions equations, where n is usually 10–20. The procedure involved in producing e-diesel is presented in Fig. 9.

$$(2n + 1)H_2 + nCO \rightarrow CnH_{2n+2} + H_2O\ \Delta H_r = n(-146)\ \text{kJ/mol} \quad (5)$$

Direct hydrogenation of CO_2 to alkanes allows for the direct use of CO_2 and H_2 (from electrolysis) [48], however, research on this topic is still in its early stages [76]. To mimic the syngas configuration of conventional coal/NG FT plants, the real plants that are now in operation rely on the conversion of CO_2 to CO [57]. As shown in little planned/current pilot plants, a CO_2 transference might be achieved in an electrolysis or reverse water gas shift (RWGS) reactor [15], [122]. The generation of e-diesel via FT synthesis, which begins with electrolytic H_2, has an efficiency factor ranging from 0.82 to 0.83 [51]. This is less than other e-fuel methods because of the intricate advancement procedure. However, with regard to its refuelling network, onboard use and logistics, e-diesel is the most "transparent" e-fuel. Simply said, e-diesel could be used in place of present fossil fuel in ICE cars and gas stations [95].

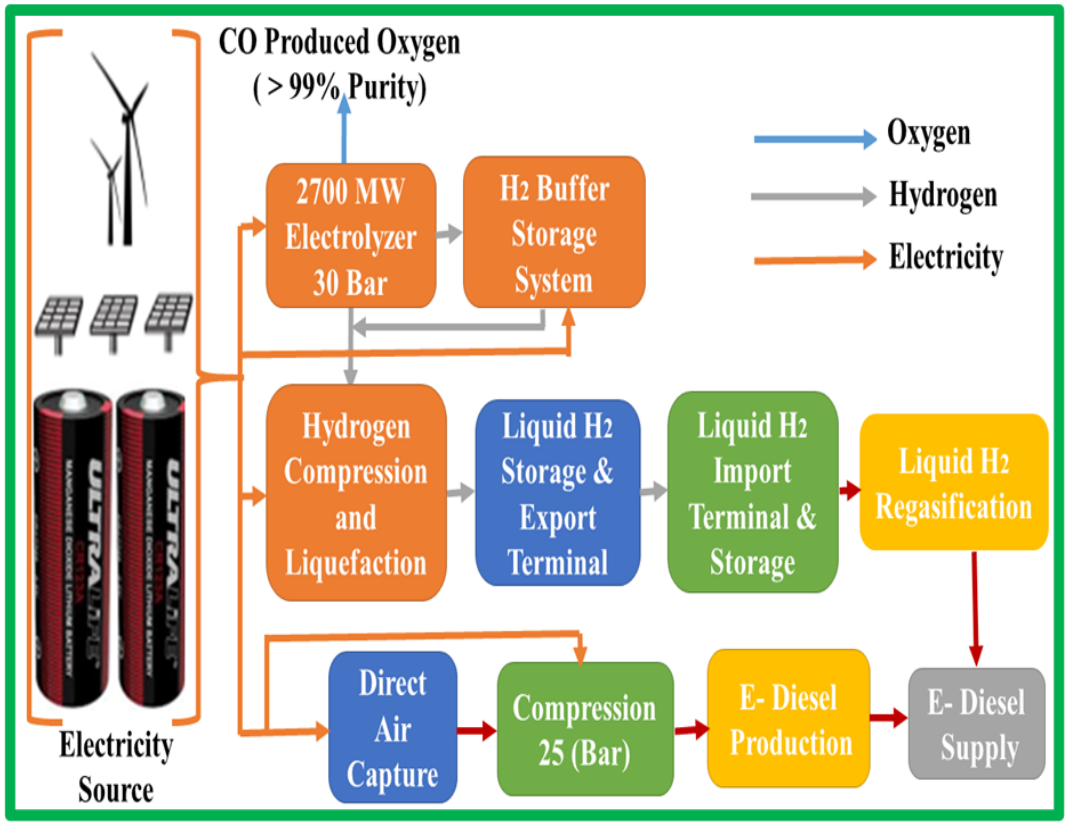

Fig. 9. The e-diesel production processes.

4.4 E-Ammonia

NH_3 has attracted a lot of attention lately since it is thought to be an efficient energy carrier and alternative fuel [127]. Fig. 10 displays the e-ammonia fabrication route. Although ammonia is used for a variety of purposes, agricultural fertilisers account for about 80% of its yearly output [128]. In addition, ammonia is a crucial feedstock for the production of other compounds, including polymers, explosives, synthetic fibres and resins, and refrigerants [128]. It shares many of the same uses as methanol, including as a synthetic fuel for gas turbines, ICE and diesel engines [128]. It can also be used as a chemical storing medium for renewable energy [129]. Nowadays, catalytic steam restructuring of natural gas produces the majority of ammonia (approximately 98%) by conventional methods. Approximately 1.8% of the world's CO_2 emissions come from this [129]. Industrial hydrogen production involves steam reformation of methane, which is subsequently introduced into the Haber-Bosch process for ammonia synthesis, which causes the reaction as shown in equation 6. The Haber-Bosch process is employed for the synthesis of ammonia (NH_3), wherein hydrogen, often generated through the

improving of natural gas, has a reaction with nitrogen under conditions of 400–450 °C and 150–200 bar of pressure, facilitated by an iron catalyst.

Overall: $3H_2(g) + N_2(g) \rightarrow 2NH_3(l)\ \Delta H_r = -91.8$ kJ/mol (6)

Much like methanol, most of the fossil fuels used to produce ammonia nowadays include coal, heavy fuel oil, natural gas and naphtha [130]. This kind of ammonia is called brown ammonia, whereas blue ammonia is ammonia made from fossil fuels with the use of CCS. Specifically, nitrogen and blue hydrogen from natural gas feedstocks and the CO_2 by-products from steam revolutionising are composed and kept, and used to make blue ammonia. In comparison to grey ammonia, this results in a decrease in climatic impact. Green ammonia is created using biomass-based hydrogen or water electrolysis, both of which have net zero emissions.

NH_3 could be used as a chemical feedstocks, pure burning fuel for vehicles, a power source (direct combustion, such as a gas turbine or fuel cell) and manufacturing processes such as the manufacturing of steel, cement and fertiliser. Ammonia is a great substitute fuel that is free of carbon and has the ability to store hydrogen. This is because ammonia has advantageous properties, such as a high hydrogen content and a tendency to liquefy in moderate temperatures [131]. In addition, with an established distribution infrastructure, ammonia storage is not too difficult [131]. The ability to store energy helps maintain a periodic equilibrium between supply and demand, which benefits structural investments and eliminates the necessity to use fossil fuels to generate electricity [132].

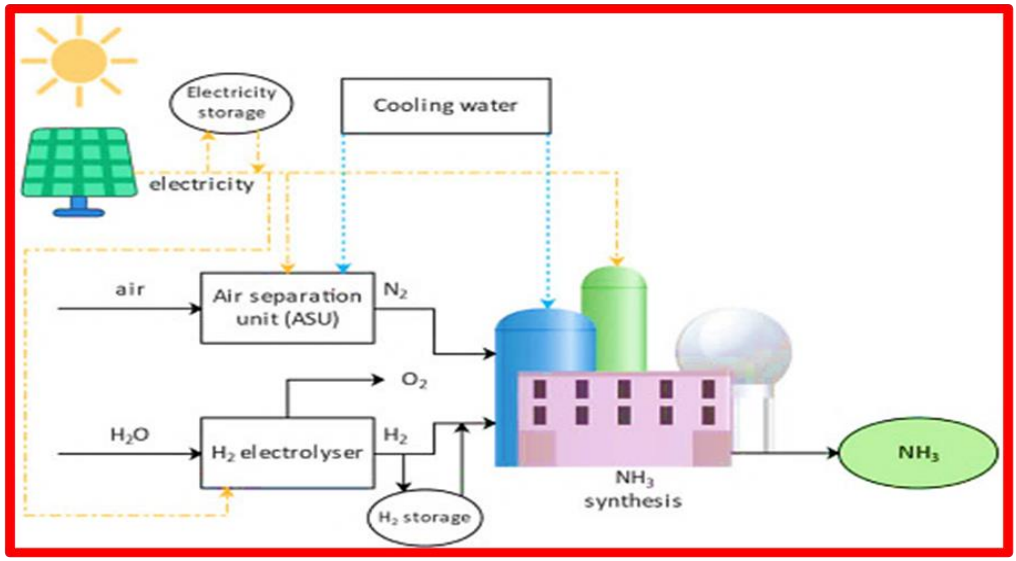

Fig. 10. Fabrication route of e-ammonia (adapted with permission from [133]).

4.5 E-Dimethyl Ether

A synthetic substitute for diesel that can be used in specifically made compression ignition diesel engines (CIDEs) is called dimethyl ether (DME). DME is a colourless gas in an ambient atmosphere. It is widely used as an aerosol propellant and in the chemical sector. DME might be produced straight using syngas as e-diesel in FT methods, employing two feasible reactions ways namely equations 7 and 8 respectively [134].

$$\text{Overall 1: } 3CO + 3H_2 \rightarrow CH_3OCH_3 + CO_2 \ \Delta H_r = -246 \text{ kJ/mol} \quad (7)$$

$$\text{Overall 2: } 2CO + 4H_2 \rightarrow CH_3OCH_3 + HO_2 \ \Delta H_r = -205 \text{ kJ/mol} \quad (8)$$

Another technique is by first synthesising methanol by means of syngas, that is $CO + H_2$ (equation 9) [134]. Second, DME is produced by dehydrating the synthesised methanol as stipulated by equation 10 [134]. The two-step reactions are presented as follows:

First stage (methanol synthesis)

$$\text{Overall 1: } CO + 2H_2 \leftrightharpoons CH_3OH \ \Delta H_r = -90.6 \text{ kJ/mol} \quad (9)$$

Second stage (methanol dehydration)

$$\text{Overall 2: } CH_3OH \leftrightharpoons CH_3OH + HO_2 \ \Delta H_r = -23.4 \text{ kJ/mol} \quad (10)$$

DME'S near-zero particle emission during burning, which is affected by its $CH_3{-}O{-}CH_3$ chemical structure and approximately 35 weight per cent oxygen content, is a promising alternative fuel for internal combustion engines (ICEs). DME is quickly atomised and has a higher cetane number. For burning methods such as homogeneous compression charge ignition (HCCI) [135], this benefit is exceedingly helpful. DME has safe storage, Azizi *et al.* [136] therefore claim that it is regarded as an alternative and clean fuel. This is owing to the ether's inability to produce explosive peroxide. DME only includes approximately 35% oxygen, and only has CH and CO bonds; CC bonds are absent. In addition, compared to natural gas, the emissions of combustion products including CO and unburned hydrocarbons are lower [137]. DME can be used in infrastructure for storage and transportation because it has a vapour pressure that is comparable to that of LPG. DME is seen as a viable alternative fuel because of its high cetane number, which prevents harmful gasses and particulate matter from being released during combustion [138].

The issues with constrained working environments and extremely subpar anti-knock efficacy are the drawbacks of DME. As a result, DME-fuelled engines encounter serious issues with novel combustion technologies such as the HCCI mode [135]. This fuel type also has poor liquid density and viscosity, small heating rate and necessitates engine amendment [139], among other significant issues. Since the reduced calorific value per

unit volume is nearly half that of diesel fuel, the DME injection quantity rate must be doubled. DME can be produced from a variety of raw materials, such as biomass (by means of the methanol dehydration reaction), coal and natural gas [140]. The third method for creating DME that was presented makes use of synthetic gases made from waste paper fluid (black liquor) from a paper industry and biomass derived from wood, such as leftover wood, including thinning wood [141].

As an alternative fuel, DME possesses qualities that meet the fuel's requirements. Its cetane number is 55–60, which is greater than diesel fuels [142]. Since DME is a gas at room temperature and 1.0 atmospheric pressure, high-pressure fuel hoses were substituted for the standard fuel hoses in the engine fuel injection set-up [134]. DME is an intriguing replacement fuel with a small boiling value of 248 K at 100 kPa and a high vapour pressure of 510 kPa at 293 K when saturated [143]. Similar reasoning was provided in the other reference, which stated that DME has an excessively high vapour pressure of 510 kPa at 293.15 K at about 25 °C [134]. This can lead to a resilient flash boiling propensity in the injection spray at low neighbouring pressure, which can enhance the break-up of DME droplets and the evaporation process mechanism [143]. Pedersen *et al.* [144], clarifies that DME is a gas at normal temperature, with a vapour pressure of about 6 bar. Here, two latent heats associated with DME exist; the latent heat of evaporation when the phase transitions from liquid to gas and the latent heat of fusion when the phase transitions from solid to liquid [134]. Approximately 4.94 kJ/mol of latent heat of fusion and 21.5 kJ/mol of latent heat of evaporation exists per mole [134].

4.6 E-Methane

Apart from non-negligible biologic output, which mostly comes from the anaerobic digestion of biomasses, methane is the primary constituent of fossil natural gas and comes from this source. However, methane can also be produced by hydrogenating CO_2. Methane (CH_4) is certainly available in nature because it makes up the bulk of ordinary gas [145]. Fig. 11 represents methane fabrication routes. Despite being one of the most significant greenhouse gases, it is used in many aspects of daily life, including ovens, water heaters, kilns, cars and other equipment, and also in industrial chemical processes and the production of power through its burning as fuel in gas turbine or steaming engines [145].

CH_4 is regarded more as an uncontaminated fuel than other hydrocarbon fuels since it releases less carbon dioxide into the atmosphere [145]. Methane absorbs larger heating per molecules matched to CO_2 because it possess a globally heating propensity (GHP) quantity of 28 on a 100 year timeline [146]. CO_2 and $4H_2$ can combined to create methane via the Sabatier technique, a direct mixture of CO reactions and the water gas shifts (WGS) reactions, as shown in equation 11 [147].

$$\text{Overall 1: } 4H_2 + CO_2 \rightarrow CH_4 + 2HO_2 \; \Delta H_r = -165 \text{ kJ/mol} \quad (11)$$

Operating within the temperature and pressure ranges of 250 to 400 °C and 5 to 50 bars correspondingly, the catalytic procedure is extremely exothermic [148]. Despite being easy to understand, this process needs a lot of CO_2 (5.5 kg for every kilogram of H_2), seems hard to come by because CCS arrangements are typically positioned far with the renewable energy sources, which raises the expense of CO_2 transportation [148]. The majority of methane is now formed cheaply using fossil fuel founded source (gray and brown methane), much like methanol and ammonia. Power to methane ($PtCH_4$) demonstration programmes, which are currently underway in numerous nations, have prompted extensive research into the CO_2 hydrogenation (methanation) pathway [149]. If H_2 is created by water electrolysis employing renewable electricity, the power to e-methane path is regarded as sustainable and renewable with decreased greenhouse gas radiations (green e-methane).

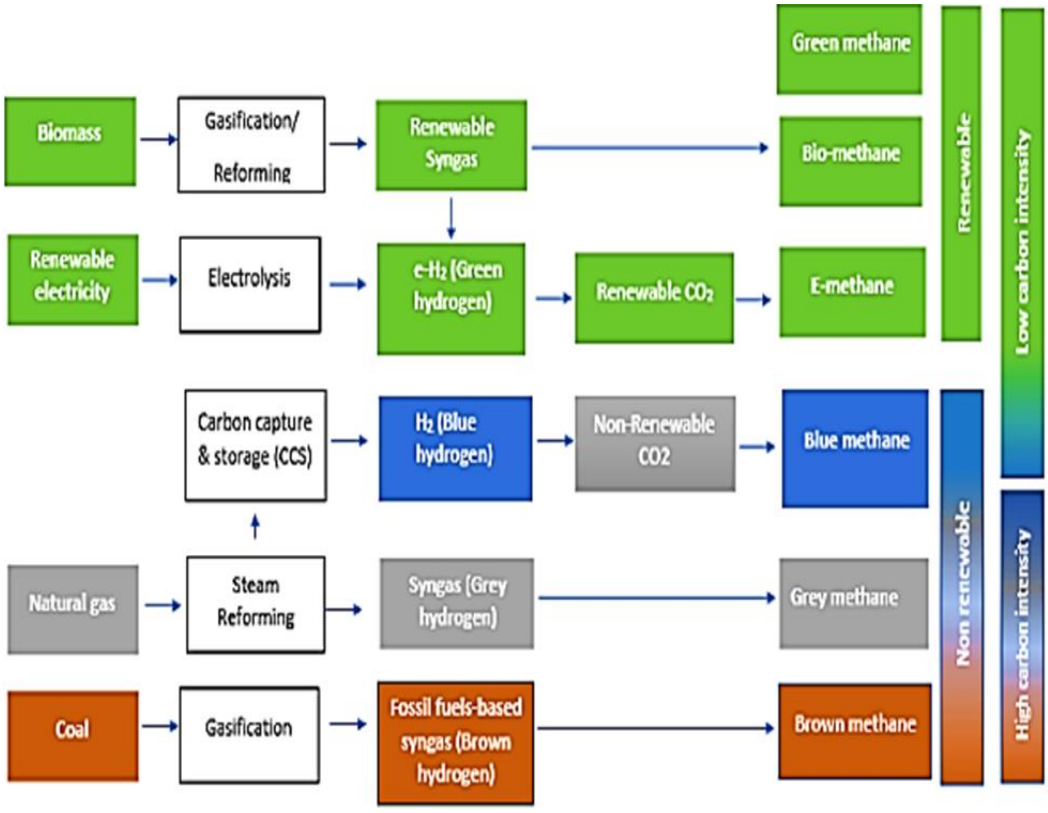

Fig. 11. Methane fabrication paths (copied with permission from [150]).

4.7 E-Kerosene

E-kerosene denotes a subgroup of e-fuels appropriate for aviation and is produced by merging hydrogen (H_2) and carbon (IV) oxide (CO_2) [151]. There exist multiple

approaches for transforming CO_2 and H_2 into liquid fuels, which consist primarily of hydrocarbons, by using biological, catalytic, electrochemical or a blend of these methods. Most experimental analyses are devoted to maximising the fabrication progression of small chain compounds such as CO, methane, methanol, acetic acid and C_2–C_4 (olefins), because of their thermodynamic constancy and chemical apathy of CO_2 [151]. These methods for the fabrication of synthetic kerosene are therefore based on multistage routes where CO_2 is first transformed into an intermediate chemical in one or more processes, and then that intermediate product serves as the feedstock for the synthesis of liquid hydrocarbons [151]. These four distinct processes for turning collected CO_2 into synthetic kerosene by employing hydrogen show how several technical factors, including hydrogen consumption, thermal energetic efficiency and the quality of the e-kerosene generated, are evaluated in a comparative manner. These two paths hinged on the FT fabrication technique while the remaining two are based on upgrading and valorising light alcohols (methanol and ethanol) obtained from CO_2 hydrogenation. This small temperature CO transfiguration via the RWGS reaction and the high-temperature direct CO_2 conversion are based on these two pathways [151].

4.7.1 FT-Based Route

This method is used in theoretical scheme and recreation analysis to minimise needless intricacy, capable of causing issues with merging because the formation of additional organic groups such as acid, alcohol and aldehyde have little effect on the procedure as a whole [152]. This method is divided into two major category, namely, high-temperature FTS without RWGS (CO_2FT) and low-temperature Fischer-Tropsch (LTFT) synthesis [152].

4.7.1.1 CO_2FT

The few investigations that are currently available on high-temperature FT synthesis without a separate reverse water–gas shift (RWGS) reactor are restricted to experimental experiments conducted in laboratories. Fe catalysts are used in this process, which combines FT and RWGS processes in a single reactor and is known as non-methanol mediated CO_2 hydrogenation [153]. The responses taken into account include equations 12 to 14 [154], [155].

$$\text{Overall 1: } H_2 + CO_2 \leftrightharpoons CO + HO_2 \tag{12}$$

$$\text{Overall 2: } nCO + (2n + 1)H_2 \leftrightharpoons C_nH_{2n+2} + nHO_2 \tag{13}$$

$$\text{Overall 3: } nCO + 2nH_2 \leftrightharpoons C_nH_{2n} + nHO_2 \tag{14}$$

A catalyst that inhibits the generation of CH_4 must be used in conjunction with high temperatures, high pressures, and excess H_2 to achieve acceptable CO_2 conversions and C_5–C_{15} yields [153]. The current study used experimental data from an Fe-based catalyst with K acting as a promoter [153]. After being recompressed, the light gases are directed to an oligomerisation reactor, which dimerises the light olefins (C_2–C_9). The gasses and

olefins are separated from the products in a flash drum. After passing through a flash drum to extract the last of the olefins, an auto thermal reactor (ATR) receives the gases. Syngas is produced when light gases, mostly CH_4, are reformatted, which raises total conversion.

4.7.1.2 LTFT

In the investigated mechanism, the RWGS reactor first converts CO_2 to CO. The reversible, endothermic, pressure-independent conversion of CO_2 to CO is thermodynamically favoured by higher temperature. The RWGS is invariably accompanied by the exothermic, lower-temperature-high-pressure unwanted CO_2 methanation, also known as the Sabatier reaction [153].

$$\text{Overall 1: } H_2 + CO_2 \leftrightharpoons CO + HO_2 \quad (15)$$

$$\text{Overall 2: } 4H_2 + CO_2 \rightarrow CH_4 + 2HO_2 \quad (16)$$

High temperatures and low pressures are therefore needed to maximise CO generation. The products of the RWGS reactor are delivered to a flash to separate the water and then adsorbed to remove CO_2 [151]. After the syngas is compressed, LTFT synthesis converts it into hydrocarbons (LTFT). It is widely believed that only paraffins are formed when Co is used as a catalyst in LTFT, and that the water–gas shift reaction (WGSR) occurs concurrently with the primary reaction [156], [157].

$$\text{Overall 1: } nCO + (2n + 1)H_2 \leftrightharpoons C_nH_{2n+2} + nHO_2 \quad (17)$$

$$\text{Overall 2: } CO + H_2O \leftrightharpoons CO_2 + H_2 \quad (18)$$

To separate the hydrocarbons, light gases and water from the reactor product, the FT reactor is cooled and decanted. After being recompressed, the light gases are routed to an ATR and an H_2 adsorption unit. In a flash drum, the extra H_2O is extracted, and the syngas is combined with new CO_2 and H_2. The larger molecules in the hydrocarbons are broken down into lighter ones in a hydrocracker [156].

$$\text{Overall 1: } C_nH_{2n+2} + H_2 \leftrightharpoons C_nH_{2n+}2 \ (C_{24} \text{ and } C_28) \quad (19)$$

4.7.2 Light Alcohol-Based Routes

Similar to previous technique discussed, this method is also divided into two subgroups, namely methanol-based routes and the methanol-to-kerosene process.

4.7.2.1 Methanol-Based Routes

The methanol path is eminent into two sections, namely, (a) methanol fabrication and (b) methanol-to-kerosene. Consequently, beginning from clean H_2 and CO_2, syngas is formed using equation 20 [156].

Overall 1: $CO_2 + 3H_2 \leftrightharpoons CH_3OH + H_2O\ \Delta H_r = -49.2$ kJ/mol (20)

The process involves feeding CO_2 and H_2 in a multistage syngas compressor together with light gases (mostly CO_2) from the first purification column. Before being fed into the methanol reactor, the compressed gas stream is combined with recycled syngas and heated. After cooling, the reaction product partially condenses [151]. To prevent an accretion of inert gases or light synthesis by-products, a portion of the unconverted syngas is purged out of the process. To overcome the synthesis reactor's pressure decrease, the residual gas phase is compressed once more. The so-called topping column receives the liquid raw methanol, which is a mixture mostly of methanol, water and solved gases [153]. Here, the mixture's light byproducts and solved gases are extracted. The primary product is pure methanol, which is produced by feeding the methanol–water mixture into the methanol column, which creates the bottom product [151].

4.7.2.2 Methanol-to-Kerosene Procedure

The methanol-to-kerosene (MtK) process comprises dehydration, oligomerisation and hydrogenation. It is comparable to typical alcohol-to-hydrocarbon procedures [151]. Fig. 12 shows the FT and methanol-based kerosene fabrication paths. The combination of oligomerisation and dehydration determines the final product. To produce light olefins, the compressed methanol is fed into the methanol-to-oxygen (MtO) reactor. After feeding the raw olefin stream into a water separation column, the CO_2 is separated by washing it with caustic soda. The olefin stream reaches the oligomerisation unit after being further dried through a molecular sieve [153].

However, MtO wastes, mostly light alkanes, are separated by cooling the reactor product of the oligomerisation process to 40 °C [152]. A distillation column receives the liquid stream and further separates naphtha and light gases from the higher olefins to maximise the output of kerosene. To avoid an amassing of higher alkanes, a purge stream is collected and the light fraction is primarily recycled to the oligomerisation reactor [152]. Although multistage oligomerisation is also possible, it is not taken into consideration here because of the generic modelling method. After that, the column's bottom stream is fractionated and hydrogenated [151].

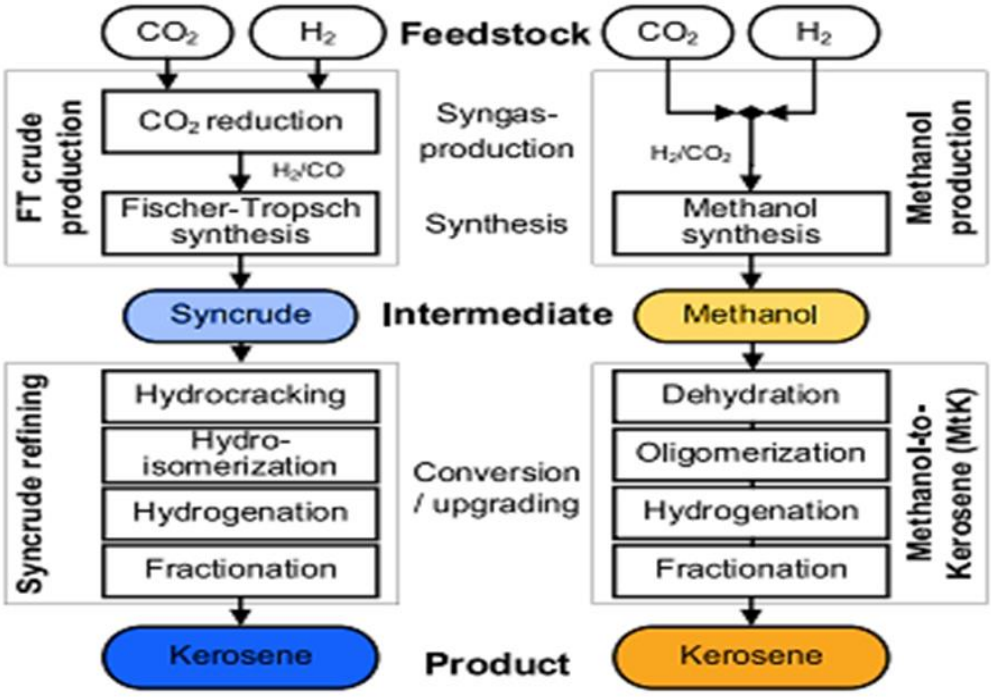

Fig. 12. Fischer-Tropsch and methanol-based kerosene production paths (copied with permission from [151]).

5 Conclusion

The impacts of using materials based on graphene in the synthesis of e-fuels from renewable energy sources are the focus of this review. In addition, it covers a few studies and initiatives that centre on the primary technologies for water electrolysis, carbon capture and transformation pathways. The three main processes of most power-to-fuel (PtF) operations are the production of power using renewable energy, the separation and hydrogenation of CO_2 into synthetic fuels using water electrolysis and CO_2 separation.

To obtain appropriate activity for e-fuel applications, defective heteroatoms and functional groups are inserted into graphene basal planes. This naturally increases the chemical and mechanical stability of the material because free graphene is stable and mechanically resilient. To achieve optimal performance, it is imperative to precisely manage the degree of graphitisation and active sites in graphene-based materials. Temperature polymer membrane-based e-fuels have been developed using graphene-based materials. The remarkable thermal resilience of graphene leads to encouraging developments in high-temperature membranes for the use of e-fuels.

Lastly, the fabrication of e-fuels, such as ammonia, methane and methanol, is encouraging especially now because e-fuels serve as exceptional energy transporters, energy storage media, fuels for various areas of application and feedstocks for chemical industries. This is in addition to the expected cost reductions of societal electricity needs, electrolysers and carbon (IV) oxide air capture. To adopt PtF technologies successfully, all obstacles and constraints must be addressed through additional research. This will be the road map in solving the task of decarbonising the environment for humankind.

6 Acknowledgements

The authors thank UNESCO, the University of South Africa and the Tertiary Education Trust Fund for their financial assistance.

7 References

[1] S. Brynolf, M. Taljegard, M. Grahn and J. Hansson, “Electrofuels for the transport sector : A review of production costs,” *Renew. Sust. Energy Rev.*, vol. 81, no. 2, pp. 1887–1905, Jan. 2018, doi: 10.1016/j.rser.2017.05.288.

[2] R. M. Obodo *et al.*, “Performance optimization of bimetallic $Co_3(PO_4)_2$@$Ni_3(PO_4)_2$ electrodes for supercapacitive applications,” *J. Mater. Sci: Mater. Electron.*, vol. 35, p. 351, Feb. 2024, doi: 10.1007/s10854-024-12079-5.

[3] R. M. Obodo *et al.*, “Evaluation of 8.0 MeV Carbon (C^{2+}) Irradiation Effects on Hydrothermally Synthesized Co_3O_4−CuO−ZnO@GO Electrodes for Supercapacitor Applications,” *Electroanalysis*, vol. 32, no. 12, pp. 2958–2968, Dec. 2020, doi: 10.1002/elan.202060382.

[4] M. Maaza *et al.*, “Peculiar Size Effects in Nanoscaled Systems,” *Nano-Horizons*, vol. 1, no. 1, pp. 1–36, Jul. 2022, doi: 10.25159/NanoHorizons.9d53e2220e31.

[5] U. R. Farooqui, A. L. Ahmad and N. Hamid, “A graphene oxide: A promising membrane material for fuel cells,” *Renew. Sustain. Energy Rev.*, vol. 82, no. 1, pp. 714–733, Feb. 2018, doi: 10.1016/j.rser.2017.09.081.

[6] A. C. Nkele *et al.*, “Recent Advances in Materials for Supercapacitors,” *Nano-Horizons*, vol. 1, no. 1, pp. 1–32, Sept. 2022, doi: 10.25159/NanoHorizons.53db1f5bd625.

[7] S. R. Chowdhury and T. Maiyalagan, “Enhanced Electro-catalytic Activity of Nitrogen-doped Reduced Graphene Oxide Supported PdCu Nanoparticles for Formic Acid Electro-oxidation,” *International Journal of Hydrogen Energy*, vol. 44, no. 29, pp. 14808–14819, Jun. 2019, doi: 10.1016/j.ijhydene.2019.04.025.

[8] R. M. Obodo *et al.*, “Annealing optimization of graphitized Co_3O_4@CuO@NiO composite electrodes for supercapacitor applications,” *Energy Storage*, vol. 4, no. 5, p. e347, Oct. 2022, doi: 10.1002/est2.347.

[9] R. M. Obodo *et al*., "Enhancement of synergistic effects of Cu_2O@MnO_2@NiO using *Sarcophrynium Brachystachys* leaf extract for supercapacitor electrode application," *Next Mater.*, vol. 5, p. 100244, Oct. 2024, doi: 10.1016/j.nxmate.2024.100244.

[10] R. M. Obodo *et al.*, "Exploring dual synergistic effects of CeO_2@ZnO mediated sarcophrynium brachystachys leaf extract nanoparticles for supercapacitor electrodes applications," *Hybrid Adv.*, vol. 5, p. 100143, Apr. 2024, doi: 10.1016/j.hybadv.2024.100143.

[11] M. Liu, R. Zhang and W. Chen, "Graphene-Supported Nanoelectrocatalysts for Fuel Cells: Synthesis, Properties, and Applications," *Chem. Rev.*, vol. 114, no. 10, pp. 5117–5160, Mar. 2014, doi: 10.1021/cr400523y.

[12] R. M. Obodo, A. C. Nwanya, I. Ahmad, M. A. Kebede and F. I. Ezema, "Carbon Derivatives in Performance Improvement of Lithium-Ion Battery Electrodes," in *Electrode Materials for Energy Storage and Conversion*, M. A. Kebede and F. I. Ezema, Eds., Boca Raton, Florida, US: CRC Press, 2021, pp. 23–33.

[13] P. H. Huang, J. K. Kuo, W. Z. Jiang and C. B. Wu, "Simulation analysis of hydrogen recirculation rates of fuel cells and the efficiency of combined heat and power," *Int. J. Hydrogen Energy*, vol. 46, no. 31, pp. 16823–16835, May 2020, doi: 10.1016/j.ijhydene.2020.08.010.

[14] R. M. Obodo, A. C. Nwanya, I. S. Ike, I. Ahmad and F. I. Ezema, "Role of Carbon Derivatives in Enhancing Metal Oxide Performances as Electrodes for Energy Storage Devices," in *Chemically Deposited Nanocrystalline Metal Oxide Thin Films*, F.I. Ezema, C. D. Lokhande and R. Rose, Eds., Cham, US: Springer, Jun. 2021, pp. 469–488, doi: 10.1007/978-3-030-68462-4_18.

[15] A. Ghosh and A. Verma, "Carbon-Polymer Composite Bipolar Plate for HT-PEMFC," *Fuel Cells*, vol. 14, no. 2, pp. 259–265, Apr. 2014, doi: 10.1002/fuce.201300186.

[16] R. M. Obodo *et al.*, "Tailoring the coexistence of $Ce(PO_4)$@$Mn_3(PO_4)_2$/MXene for supercapacitive application," *Physica Scripta*, vol. 99, no. 12, pp. 125904, Oct. 2024, doi: 10.1088/1402-4896/ad881a.

[17] R. J. Conrado, C. A. Haynes, B. E. Haendler and E. J. Toone, "Electrofuels: A New Paradigm for Renewable Fuels," in *Advanced Biofuels and Bioproducts*, J. Lee, Ed., New York, NY: Springer, 2013, pp. 1037–1064, doi: 10.1007/978-1-4614-3348-4_38.

[18] S. Li, C. Cheng and A. Thomas, "Carbon-Based Microbial-Fuel-Cell Electrodes: From Conductive Supports to Active Catalysts," *Adv. Mater.*, vol. 29, no. 8, p. 1602547, Feb. 2017, doi: 10.1002/adma.201602547.

[19] J. O. Jensen, A. P. Vestbø, Q. Li and N. J. Bjerrum, "The energy efficiency of onboard hydrogen storage," *J. Alloys Compd*, vol. 446–447, pp. 723–728, Oct. 2007, doi: 10.1016/j.jallcom.2007.04.051.

[20] R. M. Obodo *et al.*, "Investigating the dual synergistic amalgamation of CeO_2@WO_3/GO electrodes for supercapacitor application," *Energy Storage*, vol. 6, no. 5, p. e70020, Aug. 2024, doi: 10.1002/est2.70020.

[21] J. Xia *et al*., "High-performance anode material based on S and N co-doped graphene/iron carbide nanocomposite for microbial fuel cells," *J. Power Sources*, vol. 512, p. 230482, Nov. 2021, doi: 10.1016/j.jpowsour.2021.230482.

[22] B. K. Kakati, A. Ghosh and A. Verma, "Efficient composite bipolar plate reinforced with carbon fiber and graphene for proton exchange membrane fuel cell," *Int. J. Hydrogen Energy*, vol. 38, no. 22, pp. 9362–9369, Jul. 2012, doi: 10.1016/j.ijhydene.2012.11.075.

[23] R. M. Obodo *et al.*, "Effects of copper ion irradiation on $Cu_yZn_{1-2y-x}Mn_y$/GO supercapacitive electrodes," *J. Appl. Electrochem.*, vol. 51, pp. 829–845, Mar. 2021, doi: 10.1007/s10800-021-01543-3.

[24] H. Su and Y. H. Hu, "Recent advances in graphene-based materials for fuel cell applications," *Energy Sci. Eng*., vol. 9, no. 7, pp. 958–983, Jul. 2020, doi: 10.1002/ese3.833.

[25] X. Jiang and L. T. Drzal, "Exploring the potential of exfoliated graphene nanoplatelets as the conductive filler in polymeric nanocomposites for bipolar plates," *J. Power Sources*, vol. 218, pp. 297–306, Nov. 2012, doi: 10.1016/j.jpowsour.2012.07.001.

[26] R. M. Obodo *et al.*, "Radiations Induced Defects in electrode materials for energy storage devices," *Radiat. Phys. and Chem.*, vol. 191, p. 109838, Feb. 2022, doi: 10.1016/j.radphyschem.2021.109838.

[27] A. Iwan, M. Malinowski and G. Pasciak, "Polymer fuel cell components modified by graphene: Electrodes, electrolytes and bipolar plates," *Renew. Sustain. Energy Rev.*, vol. 49, pp. 954–967, Sept. 2015, doi: 10.1016/j.rser.2015.04.093.

[28] H. Huang *et al.*, "Graphene Nanoarchitectonics: Recent Advances in Graphene-Based Electrocatalysts for Hydrogen Evolution Reaction," *Adv. Mater.*, vol. 31, no. 48, p. e1903415, Nov. 2019, doi: 10.1002/adma.201903415.

[29] B. C. H. Steele and A. Heinzel, "Materials for fuel-cell technologies," *Nature*, vol. 414, pp. 345–352, Nov. 2001, doi: 10.1038/35104620.

[30] X. Zhou, J. Qiao, L. Yang and J. Zhang, "A review of graphene-based nanostructural materials for both catalyst supports and metal-free catalysts in PEM fuel cell oxygen reduction reactions," *Adv. Energy Mater.*, vol. 4, no. 8, p. 1301523, Jun. 2014, doi: 10.1002/aenm.201301523.

[31] Y. Zhu *et al.*, "Graphene and Graphene Oxide: Synthesis, Properties, and Applications," *Adv. Mater.*, vol. 22, no. 35, pp. 3906–3924, Sept. 2010, doi: 10.1002/adma.201001068.

[32] S. Navalon, A. Dhakshinamoorthy, M. Alvaro and H. Garcia, "Carbocatalysis by Graphene-Based Materials," *Chem. Rev.*, vol. 114, no. 12, pp. 6179–6212, May 2014, doi: 10.1021/cr4007347.

[33] S. S. Siwal, S. Thakur, Q. B. Zhang and V. K. Thakur, "Electrocatalysts for electrooxidation of direct alcohol fuel cell: Chemistry and applications," *Mater. Today Chem.*, vol. 14, p. 100182, Dec. 2019, doi: 10.1016/j.mtchem.2019.06.004.

[34] J. Bai, D. Liu, J. Yang and Y. Chen, "Nanocatalysts for Electrocatalytic Oxidation of Ethanol," *ChemSusChem*, vol. 12, no. 10, pp. 2117–2132, May 2019, doi: 10.1002/cssc.201803063.

[35] R. Yadav, A. Subhash, N. Chemmenchery and B. Kandasubramanian, "Graphene and Graphene Oxide for Fuel Cell Technology," *Ind. Eng. Chem. Res.*, vol. 57, no. 29, pp. 9333–9350, Jun. 2018, doi: 10.1021/acs.iecr.8b02326.

[36] R. S. Singh, A. Gautam and V. Rai, "Graphene-based bipolar plates for polymer electrolyte membrane fuel cells," *Front. Mater. Sci.*, vol. 13, no. 3, pp. 217–241, Sept. 2019, doi: 10.1007/s11706-019-0465-0.

[37] R. M. Obodo *et al.*, "Probing the performance of Co-precipitated $Co_3(PO_4)_2$@$W_3(PO_4)_4$/GO electrodes for supercapacitor application," *Mater. Chem. Phys.*, vol. 328, p. 129906, Dec. 2024, doi: 10.1016/j.matchemphys.2024.129906.

[38] J. Mergel, M. Carmo and D. Fritz, "Status on Technologies for Hydrogen Production by Water Electrolysis," in *Transition to Renewable Energy Systems*, D. Stolten and V. Scherer, Eds., Riley, 2013, ch. 22. pp. 423–450, doi: 10.1002/9783527673872.ch22.

[39] J. Vergara, C. McKesson and M. Walczak, "Sustainable energy for the marine sector," *Energy Policy*, vol. 49, pp. 333–345, Oct. 2012, doi: 10.1016/j.enpol.2012.06.026.

[40] F. Mohseni, Power to Gas- Bridging Renewable Electricity to the Transport Sector Technology. Sweden: KTH Royal Institute of Stockholm, 2012.

[41] T. Maria, B. Selma, H. Julia, H. Roman, G. Maria and A. Karin, *Electrofuels—A Possibility for Shipping in a Low Carbon Future?* Sweden: Swedish Environmental Research Institute, Stockholm, 2015.

[42] D. Wen, "Nanofuel as a potential secondary energy carrier," *Energy Environ. Sci*, vol. 3, no. 5, pp. 591–600, Feb. 2010, doi: 10.1039/b906384f.

[43] Y. Jiao, Y. Zheng, M. Jaroniec and S. Z. Qiao, "Design of electrocatalysts for oxygen- and hydrogen-involving energy conversion reactions," *Chem. Soc. Rev*., vol. 44, no. 8, pp. 2060–2086, Feb. 2015, doi: 10.1039/C4CS00470A.

[44] Q. Li, R. Cao, J. Cho and G. Wu, "Nanocarbon Electrocatalysts for Oxygen Reduction in Alkaline Media for Advanced Energy Conversion and Storage," *Adv. Eng. Mater.*, vol. 4, no. 6, p. 1301415, Apr. 2014, doi: 10.1002/aenm.201301415.

[45] L. Juha, "E-Fuel project is a collaborative act towards sustainable transportation fuels," 7 July 2021. Accessed: 29 March 2024. [Online]. Available: https://www.e-fuel.fi/about/

[46] J. Liu, Y. Qiao, C. X. Guo, S. Lim, H. Song and C. M. Li, "Graphene/carbon cloth anode for high-performance mediatorless microbial fuel cells," *Bioresour. Technol.*, vol. 114, pp. 275–280, Jun. 2012, doi: 10.1016/j.biortech.2012.02.116.

[47] G. Reiter and J. Lindorfer, "Evaluating CO_2 sources for power-to-gas applications—A case study for Austria," *J. CO2 Util.*, vol. 10, pp. 40–49, June 2015, doi: 10.1016/j.jcou.2015.03.003.

[48] P. Madejski, K. Chmie, N. Subramanian and T. Kuś, "Methods and Techniques for CO_2 Capture: Review of Potential Solutions and Applications in Modern Energy Technologies," *Energies*, vol. 15, no. 3, p. 887, 2022, doi: 10.3390/en15030887.

[49] K. Damen, M. van Troost, A. Faaij and W. Turkenburg, "A comparison of electricity and hydrogen production systems with CO_2 capture and storage—Part B: Chain analysis of promising CCS options," *Prog. Energy Combust. Sci.*, vol. 33, no. 6, pp. 580–609, Dec. 2007, doi: 10.1016/j.pecs.2007.02.002.

[50] T. Kuramochi, A. Ramírez, W. Turkenburg and A. Faaij, "Comparative assessment of CO_2 capture technologies for carbon-intensive industrial processes," *Prog. Energy Combust. Sci.*, vol. 38, pp. 87–112, Feb. 2012, doi: 10.1016/j.pecs.2011.05.001.

[51] G. Reiter and J. Lindorfer, "Evaluating CO_2 sources for power-to-gas applications–A case study for Austria," *J. CO2 Util.*, vol. 10, pp. 40–49, Jun. 2015, doi: 10.1016/j.jcou.2015.03.003.

[52] J. Zhang and L. Dai, "Nitrogen, Phosphorus, and Fluorine Tri-doped Graphene as a Multifunctional Catalyst for Self-Powered Electrochemical Water Splitting," *Angew. Chem. Int. Ed. Engl.*, vol. 55, no. 42, pp. 13296–13300, Oct. 2016, doi: 10.1002/anie.201607405.

[53] S. Fan, Li, X. Wang, C. Gua and J. Tu, "Metal oxide/hydroxide-based materials for supercapacitors," *RSC Adv.*, vol. 4, no. 79, pp. 41910–41921, Aug. 2014, doi: 10.1039/C4RA06136E.

[54] L. M. Mallard, M. A. Pimenta, G. Dresselhaus and M. S. Dresselhaus, "Raman spectroscopy in graphene," *Phys. Rep.*, vol. 473, no. 5–6, pp. 51–87, Apr. 2009, doi: 10.1016/j.physrep.2009.02.003.

[55] A. K. Geim and K. S. Novoselov, "The rise of graphene," *Nat. Mater.*, vol. 6, pp. 183–191, Mar. 2007, doi: 10.1038/nmat1849.

[56] L. M. Viculis, J. J. Mack and R. B. Kaner, "A Chemical Route to Carbon Nanoscrolls," *Sci.*, vol. 299, no. 5611, p. 1361, Feb. 2003, doi: 10.1126/science.1078842.

[57] C. Berger *et al*., "Ultrathin Epitaxial Graphite: 2D Electron Gas Properties and a Route toward Graphene-based Nanoelectronics," *J. Phys. Chem. B*, vol. 108, no. 52, p. 19912–19916, Dec. 2004, doi: 10.1021/jp040650f.

[58] T. A. Land, T. Michely, R. J. Behm, J. C. Hemminger and G. Comsa, "STM investigation of single layer graphite structures produced on Pt(111) by hydrocarbon decomposition," *Surf. Sci.*, vol. 264, no. 3, pp. 261–270, Mar. 1992, doi: 10.1016/0039-6028(92)90183-7.

[59] D. Chen, H. Feng and J. Li, "Graphene Oxide: Preparation, Functionalization, and Electrochemical Applications," *Chem. Rev.*, vol. 112, no. 11, pp. 6027–6053, Aug. 2012, doi: 10.1021/cr300115g.

[60] A. Ambrosi, C. K. Chua, A. Bonanni and M. Pumera, "Electrochemistry of Graphene and Related Materials," *Chem. Rev.*, vol. 114, no. 14, pp. 7150–7188, Jun. 2014, doi: 10.1021/cr500023c.

[61] K. S. Novoselov *et al*., "Electric Field Effect in Atomically Thin Carbon Films," *Sci.*, vol. 306, no. 5696, pp. 666–669, Oct. 2004, doi: 10.1126/science.1102896.

[62] Z. Sun and Y. H. Hu, "How Magical is Magic-Angle Graphene?," *Matter*, vol. 2, no. 5, pp. 1106–1114, May 2020, doi: 10.1016/j.matt.2020.03.010.

[63] Y. Fei, S. Fang and Y. H. Hu, "Synthesis, properties and potential applications of hydrogenated graphene," *Chem. Eng. J*., vol. 397, p. 125408, Oct. 2020, doi: 10.1016/j.cej.2020.125408.

[64] Z. Sun, S. Fang and Y. H. Hu, "3D Graphene Materials: From Understanding to Design and Synthesis Control," *Chem. Rev.*, vol. 120, no. 18, pp. 10336–10453, Aug. 2020, doi: 10.1021/acs.chemrev.0c00083.

[65] H. Sun *et al*., "Hierarchical 3D electrodes for electrochemical energy storage," *Nat. Rev. Mater.*, vol. 4, no. 1, pp. 45–60, Dec. 2018, doi: 10.1038/s41578-018-0069-9.

[66] C. Deepa, L. Rajeshkumar and M. Ramesh, "Preparation, synthesis, properties and characterization of graphene-based 2D nano-materials for biosensors and bioelectronics," *J. Mater. Res. Technol.*, vol. 19, pp. 2657–2694, Aug. 2022, doi: 10.1016/j.jmrt.2022.06.023.

[67] J. Lee, S. Noh, N. D. Pham and J. H. Shim, "Top-down synthesis of S-doped graphene nanosheets by electrochemical exfoliation of graphite: Metal-free bifunctional catalysts for oxygen reduction and evolution reactions," *Electrochim. Acta*, vol. 313, pp. 1–9, Aug. 2012, doi: 10.1016/j.electacta.2019.05.015.

[68] V. B. Mbayachi, E. Ndayiragije, T. Sammani, S. Taj and E. R. Mbuta and A. Ullah Khan, "Graphene synthesis, characterization and its applications: A review," *Res. Chem.*, vol. 3, p. 100163, Jan. 2021, doi: 10.1016/j.rechem.2021.100163.

[69] R. M. Obodo *et al.*, "Optimization of MnO_2, NiO and MnO_2@ NiO electrodes using graphene oxide for supercapacitor applications," *Curr. Res. Green Sustain. Chem.*, vol. 5, p. 100345, 2022, doi: 10.1016/j.crgsc.2022.100345.

[70] B. P. Vinayan, R. Nagar, N. Rajalakshmi and S. Ramaprabhu, "Novel Platinum–Cobalt Alloy Nanoparticles Dispersed on Nitrogen-Doped Graphene as a Cathode Electrocatalyst for PEMFC Applications," *Adv. Funct. Mater.*, vol. 22, no. 16, pp. 3519–3526, Aug. 2012, doi: 10.1002/adfm.201102544.

[71] Y. Liang *et al*., "Co_3O_4 nanocrystals on graphene as a synergistic catalyst for oxygen reduction reaction," *Nature Mater.*, vol. 10, pp. 780–786, Aug. 2011, doi: 10.1038/nmat3087.

[72] Y. Zhou *et al.*, "Making ultrafine and highly-dispersive multimetallic nanoparticles in three-dimensional graphene with supercritical fluid as excellent electrocatalyst for oxygen reduction reaction," *J. Mater. Chem. A*, vol. 4, no. 47, pp. 18628–18638, 2016, doi: 10.1039/C6TA08508C.

[73] Y. Li *et al*., "Porous graphene doped with Fe/N/S and incorporating Fe_3O_4 nanoparticles for efficient oxygen reduction," *Catal. Sci. Technol.*, vol. 8, no. 20, pp. 5325–5333, 2018, doi: 10.1039/C8CY01328D.

[74] X. H. Yan, R. Wu, J. B. Xu, Z. Luo and T. S. Zhao, "A monolayer graphene-Nafion sandwich membrane for direct methanol fuel cells," *J. Power Sources*, vol. 311, pp. 188–194, Apr. 2016, doi: 10.1016/j.jpowsour.2016.02.030.

[75] S. M. Holmes *et al.*, "2D Crystals Significantly Enhance the Performance of a Working Fuel Cell," *Adv. Energy Mater.*, vol. 7, no. 5, p. 1601216, Mar. 2017, doi: 10.1002/aenm.201601216.

[76] H. Su and Y. H. Hu, "Recent advances in graphene-based materials for fuel cell applications," *Energy Sci. Eng.*, vol. 9, no. 7, pp. 958–983, Jul. 2021, doi: 10.1002/ese3.833.

[77] Q. Zhang and J. Guan, "Single-Atom Catalysts for Electrocatalytic Applications," *Adv. Funct. Mater.*, vol. 30, no. 31, p. 2000768, Aug. 2020, doi: 10.1002/adfm.202000768.

[78] W. Gao *et al*., "Ozonated Graphene Oxide Film as a Proton-Exchange Membrane," *Angew. Chem. Int. Ed. Engl.*, vol. 53, no. 14, pp. 3588–3593, Apr. 2014, doi: 10.1002/anie.201310908.

[79] L. Yang *et al.*, "Carbon-Based Metal-Free ORR Electrocatalysts for Fuel Cells: Past, Present, and Future," *Adv. Mater.*, vol. 31, no. 13, p. 1804799, Mar. 2019, doi: 10.1002/adma.201804799.

[80] L. Qu, Y. Liu, J. B. Baek and L. Dai, "Nitrogen-Doped Graphene as Efficient Metal-Free Electrocatalyst for Oxygen Reduction in Fuel Cells," *ACS Nano*, vol. 4, no. 3, pp. 1321–1326, Feb. 2010, doi: 10.1021/nn901850u.

[81] J. Sun *et al.*, "Ultrathin Nitrogen-Doped Holey Carbon@Graphene Bifunctional Electrocatalyst for Oxygen Reduction and Evolution Reactions in Alkaline and Acidic Media," *Angew. Chem. Int. Ed. Engl.*, vol. 57, no. 50, pp. 16511–16515, Dec. 2018, doi: 10.1002/anie.201811573.

[82] X. Mao, G. Kour, C. Yan, Z. Zhu and A. Du, "Single Transition Metal Atom-Doped Graphene Supported on a Nickel Substrate: Enhanced Oxygen Reduction Reactions Modulated by Electron Coupling," *J. Phys. Chem. C*, vol. 123, no. 6, pp. 3703–3710, Jan. 2019, doi: 10.1021/acs.jpcc.8b12193.

[83] D. Geng *et al*., "High oxygen-reduction activity and durability of nitrogen-doped graphene," *Energy Environ. Sci.*, vol. 4, no. 3, p. 760, 2011, doi: 10.1039/c0ee00326c.

[84] L. Lai *et al*., "Exploration of the active center structure of nitrogen-doped graphene-based catalysts for oxygen reduction reaction," *Energy Environ. Sci*., vol. 5, no. 7, pp. 7936–7942, 2012, doi: 10.1039/c2ee21802j.

[85] J. Wu *et al*., "Nitrogen-Doped Graphene with Pyridinic Dominance as a Highly Active and Stable Electrocatalyst for Oxygen Reduction," *ACS Appl. Mater. Interfaces*, vol. 7, no. 27, pp. 14763–14769, Jun. 2015, doi: 10.1021/acsami.5b02902.

[86] D. H. Guo, R. Shibuya, C. Akiba, S. Saji, T. Kondo and J. Nakamura, "Active sites of nitrogen-doped carbon materials for oxygen reduction reaction clarified using model catalysts," *Sci.*, vol. 351, no. 6271, pp. 361–365, Jan. 2016, doi: 10.1126/science.aad0832.

[87] A. Zitolo *et al*., "Identification of catalytic sites for oxygen reduction in iron- and nitrogen-doped graphene materials," *Nat. Mater.*, vol. 14, no. 9, pp. 937–942, Aug. 2015, doi: 10.1038/nmat4367.

[88] Z. Yang *et al*., "Sulfur-Doped Graphene as an Efficient Metal-free Cathode Catalyst for Oxygen Reduction," *ACS Nano*, vol. 6, no. 1, pp. 205–211, Dec. 2012, doi: 10.1021/nn203393d.

[89] G. L. Chai, K. Qiu, M. Qiao, M. M. Titirici, C. Shang and Z. Guo, "Active sites engineering leads to exceptional ORR and OER bifunctionality in P,N Co-doped graphene frameworks," *Energy Environ. Sci.*, vol. 10, no. 5, pp. 1186–1195, 2017, doi: 10.1039/C6EE03446B.

[90] M. A. Molina-García and N. V. Rees, "'Metal-free' electrocatalysis: Quaternary-doped graphene and the alkaline oxygen reduction reaction," *Appl. Catal. A*, vol. 553, pp. 107–116, Mar. 2018, doi: 10.1016/j.apcata.2017.12.014.

[91] H. Lin *et al.*, "Boron, nitrogen, and phosphorous ternary doped graphene aerogel with hierarchically porous structures as highly efficient electrocatalysts for oxygen reduction reaction," *New J. Chem.*, vol. 40, no. 7, pp. 6022–6029, 2016, doi: 10.1039/C5NJ03390J.

[92] Y. Shao, Z. Jiang, Q. Zhang and J. Guan, "Progress in Nonmetal-Doped Graphene Electrocatalysts for the Oxygen Reduction Reaction," *ChemSusChem*, vol. 12, no. 10, pp. 2133–2146, May 2019, doi: 10.1002/cssc.201900060.

[93] R. M. Obodo *et al.*, "Influence of pH and annealing on the optical and electrochemical properties of cobalt (III) oxide (Co_3O_4) thin films," *Surf. Interfaces*, vol. 16, pp. 114–119, Sept. 2019, doi: 10.1016/j.surfin.2019.05.006.

[94] B. Das, S. Sagnik Das, S. Tewary, S. Bose, S. Ghosh and A. Ghosh, "Graphene Nanosheets for Fuel Cell Application," in *Advances in Nanosheets—Preparation, Properties and Applications*, K. Krishnamoorthy, Ed., IntechOpen, 2023, pp. 1–17, doi: 10.5772/intechopen.1001838.

[95] A. Ali and P. K. Shen, "Recent Progress in Graphene-Based Nanostructured Electrocatalysts for Overall Water Splitting," *Electrochem. Energy Rev.*, vol. 3, pp. 370–394, May 2020, doi: 10.1007/s41918-020-00066-3.

[96] X. K. Kong, C. L. Chen and Q. W. Chen, "Doped graphene for metal-free catalysis," *Chem. Soc. Rev.*, vol. 43, no. 8, pp. 2841–2857, 2014, doi: 10.1039/C3CS60401B.

[97] X. Qiu, T. Dong, M. Ueda, X. Zhang and L. Wang, "Sulfonated reduced graphene oxide as a conductive layer in sulfonated poly(ether ether ketone) nanocomposite membranes," *J. Membr. Sci.*, vol. 524, pp. 663–672, Feb. 2017, doi: 10.1016/j.memsci.2016.11.064.

[98] M. Perez-Page, M. Sahoo and S. M. Holmes, "Single Layer 2D Crystals for Electrochemical Applications of Ion Exchange Membranes and Hydrogen Evolution Catalysts," *Adv. Mater. Interfaces*, vol. 6, no. 7, p. 1801838, 2019, doi: 10.1002/admi.201801838.

[99] Y. Liu, L. Min, W. Zhang and Y. Wang, "High-Performance Graphene Coating on Titanium Bipolar plates in Fuel Cells via Cathodic Electrophoretic Deposition," *Coatings*, vol. 11, no. 4, p. 437, Apr. 2021, doi: 10.3390/coatings11040437.

[100] R. Plengudomkit, M. Okhawilai and S. Rimdusit, "Highly filled graphene-benzoxazine composites as bipolar plates in fuel cell applications," *Polym. Compos.*, vol. 37, no. 6, pp. 1715–1727, Jun. 2016, doi: 10.1002/pc.23344.

[101] L. Jiang, J. A. Syed, H. Lu and X. Meng, "In-situ electrodeposition of conductive polypyrrole-graphene oxide composite coating for corrosion protection of 304SS bipolar plates," *J. Alloys. Compd*, vol. 770, pp. 35–47, Jan. 2019, doi: 10.1016/j.jallcom.2018.07.277.

[102] V. Mišković-Stanković, I. Jevremović, I. Jung and K. Rhee, "Electrochemical study of corrosion behavior of graphene coatings on copper and aluminum in a chloride solution," *Carbon*, vol. 75, pp. 335–344, Aug. 2014, doi: 10.1016/j.carbon.2014.04.012.

[103] N. W. Pu *et al.*, "Graphene grown on stainless steel as a high-performance and ecofriendly anti-corrosion coating for polymer electrolyte membrane fuel cell bipolar plates," *J. Power Sources*, vol. 282, pp. 248–256, May 2015, doi: 10.1016/j.jpowsour.2015.02.055.

[104] Y. Sim *et al*., "Formation of 3D graphene–Ni foam heterostructures with enhanced performance and durability for bipolar plates in a polymer electrolyte membrane fuel cell," *J. Mater. Chem. A.*, vol. 6, no. 4, pp. 1504–1512, 2018, doi: 10.1039/C7TA07598G.

[105] H. Tateishi *et al*., "Graphene Oxide Fuel Cell," *J. Electrochem. Soc.*, vol. 160, no. 11, pp. F1175–F1178, Sept. 2013, doi: 10.1149/2.008311jes.

[106] H. Ren, H. Tian, C. L. Gardner, T. L. Ren and J. Chae, "A miniaturized microbial fuel cell with three-dimensional graphene macroporous scaffold anode demonstrating a record power density of over 10 000 W m^{-3}," *Nanoscale*, vol. 8, no. 6, pp. 3539–3547, 2016, doi: 10.1039/C5NR07267K.

[107] F. Ren *et al.*, "Clean Method for the Synthesis of Reduced Graphene Oxide-Supported PtPd Alloys with High Electrocatalytic Activity for Ethanol Oxidation in Alkaline Medium," *ACS Appl. Mater. Interfaces*, vol. 6, no. 5, pp. 3607–3614, Jan. 2014, doi: 10.1021/am405846h.

[108] K. Zhang, L. L. Zhang, X. Zhao and J. Wu, "Graphene/Polyaniline Nanofiber Composites as Supercapacitor Electrodes," *Chem. Mater.*, vol. 22, no. 4, pp. 1392–1401, Jan. 2010, doi: 10.1021/cm902876u.

[109] E. Yoo, T. Okata, T. Akita, M. Kohyama, J. Nakamura and I. Honma, "Enhanced Electrocatalytic Activity of Pt Subnanoclusters on Graphene Nanosheet Surface," *Nano Lett.*, vol. 9, no. 6, pp. 2255–2259, Apr. 2009, doi: 10.1021/nl900397t.

[110] I. Y. Jeon *et al*., "Edge-Selectively Sulfurized Graphene Nanoplatelets as Efficient Metal-Free Electrocatalysts for Oxygen Reduction Reaction: The Electron Spin Effect," *Adv. Mater.*, vol. 25, no. 42, pp. 6138–6145, Nov. 2013, doi: 10.1002/adma.201302753.

[111] C. Zhang *et al.*, " Single-Atomic Ruthenium Catalytic Sites on Nitrogen-Doped Graphene for Oxygen Reduction Reaction in Acidic Medium," *ACS Nano*, vol. 11, no. 7, pp. 6930–6941, Jun. 2017, doi: 10.1021/acsnano.7b02148.

[112] A. Ambrosi *et al*., "Graphene and its electrochemistry—an update," *Chem. Soc. Rev.*, vol. 45, no. 9, pp. 2458–2493, 2016, doi: 10.1039/C6CS00136J.

[113] L. Chang, D. J. Stacchiola and Y. H. Hu, "An Ideal Electrode Material, 3D Surface-Microporous Graphene for Supercapacitors with Ultrahigh Areal Capacitance," *ACS Appl. Mater. Interfaces*, vol. 9, no. 29, pp. 24655–24661, Jul. 2017, doi: 10.1021/acsami.7b07381.

[114] M. Matsumoto, Y. Saito, C. Park, T. Fukushima and T. Aida, "Ultrahigh-throughput exfoliation of graphite into pristine 'single-layer' graphene using microwaves and molecularly engineered ionic liquids," *Nat. Chem.*, vol. 7, no. 9, pp. 730–736, Aug. 2015, doi: 10.1038/nchem.2315.

[115] Y. Xu, K. Sheng, C. Li and G. Shi, "Self-Assembled Graphene Hydrogel *via* a One-Step Hydrothermal Process," *ACS Nano*, vol. 4, no. 7, pp. 4324–4330, Jun. 2010, doi: 10.1021/nn101187z.

[116] D. Voiry *et al.*, "High-quality graphene via microwave reduction of solution-exfoliated graphene oxide," *Sci.*, vol. 353, no. 6306, pp. 1413–1416, Sept. 2016, doi: 10.1126/science.aah3398.

[117] S. Fang, Y. Lin and Y. H. Hu, "Recent Advances in Green, Safe, and Fast Production of Graphene Oxide via Electrochemical Approaches," *ACS Sustain. Chem. Eng.*, vol. 7, no. 15, pp. 12671–12681, Jul. 2019, doi: 10.1021/acssuschemeng.9b02794.

[118] X. Li *et al.*, "Large-Area Synthesis of High-Quality and Uniform Graphene Films on Copper Foils," *Sci.*, vol. 324, no. 5932, pp. 1312–1314, May 2009, doi: 10.1126/science.1171245.

[119] H. Wang, K. Sun, F. Tao, D. J. Stacchiola and Y. H. Hu, "3D Honeycomb-Like Structured Graphene and Its High Efficiency as a Counter-Electrode Catalyst for Dye-Sensitized Solar Cells," *Angew. Chem. Int. Ed. Engl.*, vol. 52, no. 35, pp. 9210–9214, Aug. 2013, doi: 10.1002/anie.201303497.

[120] G. Leonzio, "Methanol Synthesis: Optimal Solution for a Better Efficiency of the Process," *Processes*, vol. 6, no. 3, Feb. 2018, doi: 10.3390/pr6030020.

[121] H. W. M. Madej-Lachowska, A. Kasprzyk-Mrzyk and H. Moroz, "Methanol Synthesis from Carbon Dioxide and Hydrogen over CuO/ZnO/ZrO2 promoted catalysts," *Chemik*, vol. 68, no. 1, pp. 61–68, 2014.

[122] G. A. Olah, A. Goeppert and G. K. S. Prakash, "Chemical Recycling of Carbon Dioxide to methanol and dimethyl ether: from greenhouse gas to renewable, environmentally carbon neutral fuels and synthetic hydrocarbons," *J. Org. Chem.*, vol. 74, no. 2, pp. 487–498, 2009, doi: 10.1021/jo801260f.

[123] M. Taljegård *et al.*, "Electrofuels—A Possibility for Shipping in a Low Carbon Future?," presented at the Int. Conf. on Shipping in Changing Climates, Glasgow, Scotland, 2015.

[124] M. Rivarolo, D. Bellotti, L. Magistri and A. F. Massardo, "Feasibility study of methanol production from different renewable sources and thermo-economic analysis," *Int. J. Hydrogen Energy*, vol. 41, no. 4, pp. 2105–2116, Jan. 2016, doi: 10.1016/j.ijhydene.2015.12.128.

[125] R. Kajaste, M. Hurme and P. Oinas, "Methanol-Managing greenhouse gas emissions in the production chain by optimizing the resource base," *AIMS Energy*, vol. 6, no. 6, pp. 1074–1102, Dec. 2018, doi: 10.3934/energy.2018.6.1074.

[126] M. Noussan, P. P. Raimondi, R. Scita and M. Hafner, "The Role of Green and Blue Hydrogen in the Energy Transition—A Technological and Geopolitical Perspective," *Sustainability*, vol. 13, no. 1, pp. 1–26, 2021, doi: 10.3390/su13010298.

[127] H. Stancin, H. MikuIcic, X. Wang and N. Duic, "A review on alternative fuels in future energy system," *Renew. Sustain. Energy Rev.*, vol. 128, p. 128, Aug. 2020, doi: 10.1016/j.rser.2020.109927.

[128] E. R. Morgan, J. F. Manwell and J. G. McGowan, "Sustainable Ammonia Production from U.S. Offshore Wind Farms: A Techno-Economic Review," *ACS Sustain. Chem. Eng.*, vol. 5, no. 11, pp. 9554–9567, Oct. 2017, doi: 10.1021/acssuschemeng.7b02070.

[129] M. Matzen, M. Alhajji and Y. Demirel, "Technoeconomics and Sustainability of Renewable Methanol and Ammonia Productions Using Wind Power-based Hydrogen," *J. Adv. Chem. Eng.*, vol. 5, no. 3, 2015, doi: 10.4172/2090-4568.1000128.

[130] K. H. R. Rouwenhorst, Y. Engelmann, K. Veer, R. S. Postma, A. Bogaerts and L. Lefferts, "Plasma-driven catalysis: green ammonia synthesis with intermittent electricity," *Green Chem.*, vol. 22, no. 19, pp. 6258–6287, 2020, doi: 10.1039/D0GC02058C.

[131] G. C. Funez, L. Reyes-Bozo, E. Vyhmeister, C. M. Jaen, J. L. Salazar and C. Clemente-Jul, "Technical-economic analysis for a green ammonia production plant in Chile and its subsequent transport to Japan," *Renew. Energy*, vol. 157, pp. 404–414, Sept. 2020, doi: 10.1016/j.renene.2020.05.041.

[132] R. M. Obodo *et al.*, "Improving the Supercapacitive Performance of Nanoengineered Co_3O_4@Mn_3O_4@NiO/MXene Electrode Using Ion Beam Implantation," *J. Mater. Eng. Perform.*, Dec. 2024, doi: 10.1007/s11665-024-10570-y.

[133] F. Mohammad, "Chapter 13—Ammonia production from syngas: Plant design and simulation," Advances in Synthesis Gas: Methods, Technologies and Applications. Volume 4: Syngas Process Modelling and Apparatus Simulation, Elsevier, 2023, pp. 381–399, doi: 10.1016/B978-0-323-91879-4.00012-6.

[134] P. Yanuandri and L. Ocktaeck, "Dimethyl Ether as the Next Generation Fuel to Control Nitrogen Oxides and Particulate Matter Emissions from Internal Combustion Engines: A Review," *ACS Omega*, vol. 7, pp. 32−37, Dec. 2022, doi: 10.1021/acsomega.1c03885.

[135] Y. Yan, Z. Yu-Sheng, C. Yong-Tian, C. Zu-Di and X. Ge, "Study on HCCI Combustion and Emission Characteristics of Diesel Engine Fueled with Methanol/DME," *SAE Tech. Pap. Ser.*, Jan. 2010, doi: 10.4271/2010-01-0578.

[136] Z. Azizi, M. Rezaeimanesh, T. Tohidian and M. R. Rahimpour, "Dimethyl Ether: A Review of Technologies and Production Challenges," *Chem. Eng. Process*, vol. 82, pp. 150−172, Aug. 2014, doi: 10.1016/j.cep.2014.06.007.

[137] K. Cung and S. Lee, "Numerical Study on Emission Characteristics of High-Pressure Dimethyl Ether (DME) under Different Engine Ambient Conditions," *SAE Tech. Pap. Ser*., Jan. 2013, doi: 10.4271/2013-01-0319.

[138] D. Lee, "Spray Characteristics of DME-LPG Blended Fuel in a High-Pressure Diesel Injection System," *SAE Tech. Pap. Ser*., Jan. 2013, doi: 10.4271/2013-01-0105.

[139] S. Bhattacharya, K. B. Kabir and K. Hein, "Dimethyl ether synthesis from Victorian brown coal through gasification—Current status, and research and development needs," *Prog. Energy Combust. Sci*., vol. 39, no. 6, p. 577−605, Dec. 2013, doi: 10.1016/j.pecs.2013.06.003.

[140] C. Arcoumanis, C. Bae, R. Crookes and E. Kinoshita, "The potential of di-methyl ether (DME) as an alternative fuel for compression-ignition engines: A review," *Fuel*, vol. 87, no. 7, pp. 1014−1030, 2008, doi: 10.1016/j.fuel.2007.06.007.

[141] W. Chen, B. Lin, H. Lee and M. Huang, "One-step synthesis of dimethyl ether from the gas mixture containing CO_2 with high space velocity," *Appl. Energy*, vol. 98, pp. 92−101, Oct. 2012, doi: 10.1016/j.apenergy.2012.02.082.

[142] S. Xu, Y. Wang, X. Zhang, X. Zhen and C. Tao, "Development of a novel common-rail type Dimethyl ether (DME) injector," *Appl. Energy*, vol. 94, pp. 1−12, Jun. 2012, doi: 10.1016/j.apenergy.2012.01.030.

[143] J. Yu, Y. Zhang, G. Jiang and Q. Kui, "An Experimental Study on Steady Flash Boiling Spray Characteristics of DME/Diesel Blended," *SAE Tech. Pap. Ser*., Jan. 2010, doi: 10.4271/2010-01-0879.

[144] T. D. Pedersen and J. Schramm, "Reduction of HCCI Combustion Noise Through Piston Crown Design," *SAE Tech. Pap. Ser*., Jan. 2010, doi: 10.4271/2010-01-1487.

[145] L. Guerra, S. Rossi, J. Rodrigues, J. Gomes, J. Puna and M. T. Santos, "Methane production by a combined Sabatier reaction/water electrolysis process," *J. Environ. Chem. Eng.*, vol. 6, no. 1, pp. 671–676, Feb. 2018, doi: 10.1016/j.jece.2017.12.066.

[146] J. Huang, B. Mendoza, J. S. Daniel, C. J. Nielsen, L. Rotstayn and O. Wild, "Anthropogenic and Natural Radiative Forcing," in *Climate Change 2013: The Physical Science Basis. Contribution of Working Group I to the Fifth Assessment Report of the Intergovernmental Panel on Climate Change*, T. F. Stocker *et al.*, Eds., Cambridge, United Kingdom: Cambridge University Press, 2013, pp. 659–740.

[147] G. Leonzio, "Process analysis of biological Sabatier reaction for bio-methane production," *Chem. Eng. J.*, vol. 290, pp. 490–498, Apr. 2016, doi: 10.1016/j.cej.2016.01.068.

[148] L. Wang *et al.*, "Power-to-methane via co-electrolysis of H_2O and CO_2: The effects of pressurized operation and internal methanation," *Appl. Energy*, vol. 250, pp. 1432–1445, Sept. 2019, doi: 10.1016/j.apenergy.2019.05.098.

[149] B. R. de Vasconcelos and J. M. Lavoie, "Recent Advances in Power-to-X Technology for the Production of Fuels and Chemicals," *Front. Chem.*, vol. 7, pp. 1–24, Jun. 2019, doi: 10.3389/fchem.2019.00392.

[150] A. Nemmour, A. Inayat, I. Janajreh and C. Ghenai, "Green hydrogen-based E-fuels (E-methane, E-methanol, E-ammonia) to support clean energy transition: A literature review," *Int. J. Hydrogen Energy*, vol. 48, no. 75, pp. 29011–29033, Sept. 2023, doi: 10.1016/j.ijhydene.2023.03.240.

[151] S. Bube, N. Nils Bullerdiek, S. Voß and M. Kaltschmitt, "Kerosene production from power-based syngas—A technical comparison of the Fischer-Tropsch and methanol pathway," *Fuel*, vol. 366, p. 131269, Jun. 2024, doi: 10.1016/j.fuel.2024.131269.

[152] E. Corrao *et al.*, "CO_2 conversion into hydrocarbons via modified Fischer-Tropsch synthesis by using bulk iron catalysts combined with zeolites," *Chem. Eng. Res. Des.*, vol. 197, p. 449–465, Sept. 2023, doi: 10.1016/j.cherd.2023.07.052.

[153] A. Buttler and H. Spliethoff, "Current status of water electrolysis for energy storage, grid balancing and sector coupling via power-to-gas and power-to-liquids: A review," *Renew. Sustain. Energy Rev.*, vol. 82, pp. 2440–2454, Feb. 2018, doi: 10.1016/j.rser.2017.09.003.

[154] V. Dieterich, A. Buttler, A. Hanel, H. Spliethoff and S. Fendt, "Power-to-liquid via synthesis of methanol, DME or Fischer–Tropsch-fuels: a review," *Energy Environ. Sci*, vol. 13, no. 10, pp. 3207–3252, 2020, doi: 10.1039/D0EE01187H.

[155] C. Panzone, R. Philippe, A. Chappaz, P. Fongarland and A. Bengaouer, "Power-to-Liquid catalytic CO_2 valorization into fuels and chemicals: Focus on the Fischer-Tropsch route," *J. CO2 Util.*, vol. 38, pp. 314–347, May 2020, doi: 10.1016/j.jcou.2020.02.009.

[156] J. Wei *et al.*, "Directly converting CO_2 into a gasoline fuel," *Nat. Commun.*, vol. 8, p. 15174, May 2017, doi: 10.1038/ncomms15174.

[157] J. N. Udeh *et al*., "Investigating the properties of cobalt phosphate nanoparticles synthesized by co-precipitation method," *Asian J. Nano. Mater*., vol. 5, no. 1, pp. 22–35, 2022, https://www.sid.ir/paper/1144048/en.